NUREG/CR--5581

TI91 007152

Unsaturated Flow and Transport Through Fractured Rock Related to High-Level Waste Repositories

Final Report – Phase III

Manuscript Completed: December 1990
Date Published: January 1991

Prepared by
D. D. Evans, T. C. Rasmussen

T. J. Nicholson, NRC Project Manager

Department of Hydrology and Water Resources
University of Arizona
Tucson, AZ 85721

Prepared for
Division of Engineering
Office of Nuclear Regulatory Research
U.S. Nuclear Regulatory Commission
Washington, DC 20555
NRC FIN D1662

OTHER REPORTS IN THIS SERIES

Evans, D.D., 1983, Unsaturated Flow and Transport Through Fractured Rock - Related to High-Level Waste Repositories, NUREG/CR-3206, 231 pp.

Schrauf, T.W. and D.D. Evans, 1984, Relationship Between the Gas Conductivity and Geometry of a Natural Fracture, NUREG/CR-3680, 131 pp.

Huang, C. and D.D. Evans, 1985, A 3-Dimensional Computer Model to Simulate Fluid Flow and Contaminant Transport Through a Rock Fracture System, NUREG/CR-4042, 109 pp.

Green, R.T. and D.D. Evans, 1987, Radionuclide Transport as Vapor Through Unsaturated Fractured Rock, NUREG-CR-4654, 163 pp.

Rasmussen, T.C. and D.D. Evans, 1987, Unsaturated Flow and Transport Through Fractured Rock - Related to High-Level Waste Repositories, NUREG/CR-4655, 474 pp.

Yeh, T.C.J., T.C. Rasmussen and D.D. Evans, 1988, Simulation of Liquid and Vapor Movement in Unsaturated Fractured Rock at the Apache Leap Tuff Site: Models and Strategies, NUREG/CR-5097, 73 pp.

Weber, D.S. and D.D. Evans, 1988, Stable Isotopes of Authigenic Minerals in Variably-Saturated Fractured Tuff, NUREG/CR-5255, 70 pp.

Rasmussen, T.C. and D.D. Evans, 1989, Fluid Flow and Solute Transport Modeling Through Three-Dimensional Networks of Variably Saturated Discrete Fractures, NUREG/CR-5239, 193 pp.

Chuang, Y., W.R. Haldeman, T.C. Rasmussen, and D.D. Evans, 1990, Laboratory Analysis of Fluid Flow and Solute Transport Through a Variably Saturated Fracture Embedded in Porous Tuff, NUREG/CR-5482, 328 pp.

Rasmussen, T.C., D.D. Evans, P.J. Sheets and J.H. Blanford, 1990, Unsaturated Fractured Rock Characterization Methods and Data Sets at the Apache Leap Tuff Site, NUREG/CR-5596, 139 pp.

DISCLAIMER

DISCLAIMER

Portions of this document may be illegible in electronic image products. Images are produced from the best available original document.

ABSTRACT

Research results are summarized for a U.S. Nuclear Regulatory Commission contract with the University of Arizona focusing on field and laboratory methods for characterizing unsaturated fluid flow and solute transport related to high-level radioactive waste repositories. Characterization activities are presented for the Apache Leap Tuff field site. The field site is located in unsaturated, fractured tuff in central Arizona. Hydraulic, pneumatic, and thermal characteristics of the tuff are summarized, along with methodologies employed to monitor and sample hydrologic and geochemical processes at the field site. Thermohydrologic experiments are reported which provide laboratory and field data related to the effects of non-isothermal conditions and flow and transport in unsaturated, fractured rock.

TABLE OF CONTENTS

LIST OF TABLES

LIST OF TABLES (Continued)

LIST OF FIGURES

LIST OF FIGURES (Continued)

ACKNOWLEDGEMENTS

The research results presented here resulted from a program funded by the U.S. Nuclear Regulatory Commission (USNRC) under contract number NRC-04-86-114. The USNRC project monitor was Thomas J. Nicholson. This report was compiled and written by Daniel D. Evans and Todd C. Rasmussen. Substantial laboratory and field support was provided by Priscilla Sheets and James Blanford, respectively. Contributions from the following University of Arizona faculty are acknowledged:

- Dr. James G. McCray — Dept. of Nuclear and Energy Engineering
- Dr. T.-C. Jim Yeh — Dept. of Hydrology and Water Resources
- Dr. Randy L. Bassett — Dept. of Hydrology and Water Resources

In addition, the following graduate students within the Department of Hydrology and Water Resources substantially contributed to the material presented:

- Steven Brown
- Yueh Chuang
- Bill Davies
- Alexander Elder
- Tim Goering
- Ron Green
- William Haldeman
- Elizabeth Lyons
- Kevin Myers
- Eric Rogoff
- Stuart Smith
- Todd Thornburg
- Vincent Tidwell
- Gerald Vogt
- Daniel Weber

EXECUTIVE SUMMARY

This document summarizes research results related to NRC contract NRC-04-86-114 under FIN D1662. The contract was designed to aid in the evaluation of methods used to characterize fluid flow and solute transport in unsaturated fractured geologic media, with specific reference to the disposal of high-level nuclear waste (HLW) in such media. The research results are derived from laboratory, field and numerical simulation experiments conducted to provide primary data sets and analyses with regard to processes directly related to the performance of a HLW repository. These research results were obtained over an approximate three year period, from August 1, 1986 to November 30, 1989.

The research needs which motivated the activities described in this document were identified in two symposia and peer reviews of earlier research programs (Rasmussen and Evans, 1987; Rasmussen et al., 1988). This document concentrates on the assessment of important field-scale parameters and conceptual models which will be used to understand unsaturated flow and associated contaminant movement in both the vertical and horizontal directions. Fractured materials have been characterized using laboratory and field tests to determine their interstitial, hydraulic, pneumatic, and thermal properties. The purpose of the characterization exercise is to provide data sets which can be used to meet objectives related to:

- Subsurface instrument emplacement strategies and the importance of scale effects;
- Characterization techniques for matrix and fracture systems;
- Methods to analyze flux and travel times in fracture-matrix systems;
- Appropriate computer models for vapor-liquid flow systems;
- Methods for sampling liquid and vapor in the unsaturated zone;
- Ground-water recharge, infiltration and deep percolation estimation techniques; and
- Determination of calibration strategies using ground-water chemistry.

The attainment of these objectives will result in a better understanding of processes which affect fluid flow and solute transport in unsaturated fractured media, as well as for providing assessments of data collection and interpretation procedures.

The role of characterization of unsaturated flow and transport is an important component of performance assessment, in that the ability of the proposed high-level waste repository and surrounding geologic medium to contain the waste must be evaluated with respect to individual performance parameters. Mechanisms for waste transport must be identified, and models developed to describe fracture-matrix systems, as well as liquid-vapor flow and transport.

The Apache Leap Tuff Site (ALTS), a field site located in central Arizona is being used to gather data and evaluate methods for the purpose of meeting the objectives described above and to evaluate the relative importance of unsaturated zone flow and transport processes. The site is

similar in many respects to Yucca Mountain in southern Nevada where the candidate HLW repository site is being characterized. Characterization data sets for the interstitial, hydraulic, pneumatic and thermal properties of unsaturated fractured rock collected at the Apache Leap Tuff Site are presented for laboratory experiments on core segments collected at three meter intervals, as well as for field experiments conducted over the same three meter intervals from which the core segments were collected. Interstitial properties include bulk density, porosity, and pore surface and pore area distributions. Hydraulic properties include laboratory moisture characteristic curves, saturated and relative hydraulic conductivity, and field estimates of water content and saturated hydraulic conductivity. Pneumatic properties measured are laboratory oven-dry and relative air permeability and field air permeability. Thermal properties measured are laboratory saturated and relative thermal conductivity as a function of matric suction, as well as rock heat capacity. Field thermal diffusivity is also estimated.

Comparisons of field and laboratory data demonstrate similarities as well as important differences. Laboratory data are used to obtain data sets for matrix pneumatic and hydraulic properties over a large range of water contents and matric suctions. In all cases the oven-dry air permeability exceeds the saturated water permeability, a phenomenon which can be attributed to slip flow of the gas phase. Interpreted pore sizes using the Klinkenberg analysis agree with pore size distributions obtained using mercury intrusion data. Field estimates of saturated hydraulic permeability and pneumatic permeability for ambient rock water saturations are also available for three meter borehole intervals corresponding to where the rock segments were collected. For large air and water permeabilities the air permeability exceeds the water permeability, a phenomenon which cannot be attributed to slip flow due to the large pore sizes. Air entrapment may be responsible for the discrepancy. For lower air and water permeabilities, the air permeability is lower than the water permeability due to relative fluid saturations of approximately 70 percent during the air test. Closer agreement between air and water permeabilities are obtained when the air permeability is divided by the laboratory relative air permeability obtained from core segments tested at the ambient matric suction.

For both air and water permeability a noticeable difference between field and laboratory samples occurs for a number of intervals. This difference can be attributed to the presence of fractures which were specifically excluded in the laboratory tests. Ongoing experiments to directly measure unsaturated fracture properties in the laboratory and field are currently being conducted and promise to provide additional information on unsaturated fracture fluid flow properties.

Thermal diffusivities measured in the field from the annual change in temperature with depth compare favorably with diffusivities calculated from laboratory core segments. The influence of water content changes and the presence of fractures does not appear to appreciably affect heat flux due to surface heating.

The methods and data sets related to the characterization of the interstitial, hydraulic, pneumatic, and thermal properties are reported in Rasmussen et al. (1990). Moisture-dependent fracture flow properties are reported in Chuang et al. (1990). Additional laboratory experiments have been conducted to determine the importance of fracture flow over a range of matric suctions (Myers, 1989). The fracture hydraulic parameters of interest are the saturated and unsaturated fracture transmissivity and hydraulic conductance. Fracture porosity and degree of channeling are also important characterization parameters.

Uncertainties associated with estimation of hydrologic parameters must be quantified as part of site characterization and performance assessment studies. It is shown for selected hydrologic parameters that replication is useful for estimating the relative contribution of measurement error to geologic variability. Bias associated with specific procedures are quantified using duplication and redundancy.

Field sampling and monitoring techniques are required in order to calibrate and validate computer and conceptual models. Liquid and vapor sampling techniques are presented, along with methods for evaluating ground-water recharge, infiltration, and deep percolation. Characterization of hydrologic regimes is also possible using ground-water chemistry. Samples of minerals have been collected for stable isotope analysis. These analyses can be used to evaluate relative rates of movement in fractures and the rock matrix. Sulfate concentrations near a fracture are also used to evaluate the interaction between fracture and rock matrix flow.

Thermohydrologic experiments have also been conducted. In the laboratory, unsaturated rock cores are heated on one end, while a substantially cooler temperature is maintained at the opposite end. The one-dimensional experiment under ideal conditions indicates that a zone of desiccation will develop near the heated end, and a zone of increased water content will develop near the cooler end. Solutes are observed to accumulate near the heated end of the unfractured rock core. A field thermohydrologic experiment provides additional evidence to support the laboratory observation that a zone of desiccation will occur near a heat source. Unlike the laboratory experiment, however, a zone of condensation was not observed in the rock. Water was observed to accumulate in the borehole near the heater source, however.

1. INTRODUCTION

1.1 Study Objectives

The research findings summarized in this document are motivated by NRC regulatory needs which originated in the technical review of the DOE Environmental Assessment for the Yucca Mountain Site. The Yucca Mountain site has been recommended for characterization as a high-level waste repository. Yucca Mountain is situated in southern Nevada near and partially within the Nevada Test Site. The proposed repository horizon is situated in the unsaturated zone approximately midway between the ground surface and the water table. The need to isolate high-level waste from the environment requires that engineered and geologic barriers be devised and characterized for the purpose of assuring compliance with regulatory containment criteria. The process of assuring compliance with regulatory criteria is termed Performance Assessment, and is an essential step in the licensing and design of the proposed repository.

The research needs which motivated the activities described in this document were identified in two symposia and peer reviews of earlier research programs (Rasmussen and Evans, 1987; Rasmussen et al., 1988). This document concentrates on the assessment of important field-scale parameters and conceptual models which will be used to understand unsaturated flow and associated contaminant movement in both the vertical and horizontal directions. Fractured materials have been characterized using laboratory and field tests to determine their interstitial, hydraulic, pneumatic, and thermal properties. The purpose of the characterization exercise is to provide data sets which can be used to meet objectives related to:

- Subsurface instrument emplacement strategies and the importance of scale effects;
- Characterization techniques for matrix and fracture systems;
- Methods to analyze flux and travel times in fracture-matrix systems;
- Appropriate computer models for vapor-liquid flow systems;
- Methods for sampling liquid and vapor in the unsaturated zone;
- Ground-water recharge, infiltration and deep percolation estimation techniques; and
- Determination of calibration strategies using ground-water chemistry.

The attainment of these objectives will result in a better understanding of processes which affect fluid flow and solute transport in unsaturated fractured media, as well as for providing assessments of data collection and interpretation procedures.

1.2 Field Site Description

The Apache Leap Tuff Site (ALTS), a field site located in central Arizona (Figure 1), is being used to gather data and evaluate methods for the purpose of meeting the objectives described above and to evaluate the relative importance of unsaturated zone flow and transport processes. The site is similar in many respects to Yucca Mountain in southern Nevada where

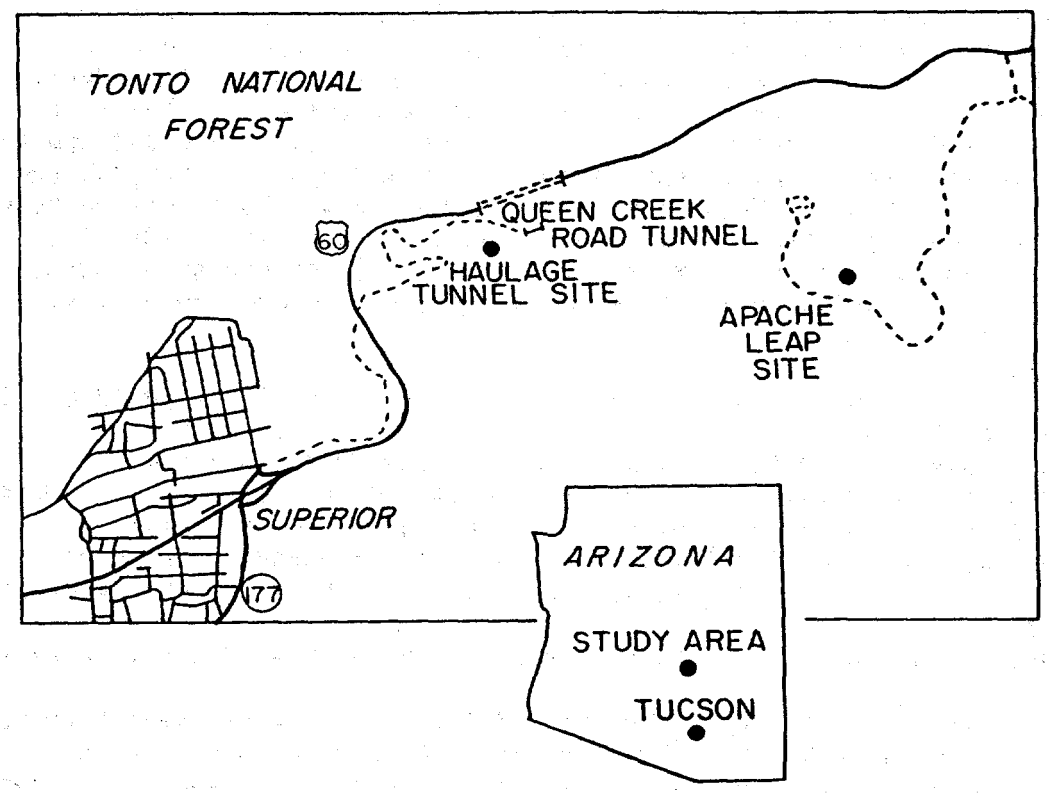

Figure 1: Location map of Apache Leap Tuff Site and surrounding area.

the candidate HLW repository site is being characterized. Table 1 presents summary data comparing selected parameters for the Apache Leap Tuff Site, White Unit, with data for the Yucca Mountain Paintbrush Tuff, Topopah Spring Member.

Table 1: Comparison of rock matrix properties. Samples obtained from the Apache Leap Tuff Site, White Unit (Source: Rasmussen et al., 1990), with selected data for Yucca Mountain Paintbrush Tuff, Topopah Spring Member (Source: Tien et al., 1985).

	ALTS White Unit		Yucca Mtn - Paintbrush Tuff Topopah Spring Member	
	mean	range	mean	range
Bulk Density ($g\ cm^{-3}$)	2.12	1.86 - 2.20	-	1.87 - 2.19
Effective Porosity (%)	17.5	13.04 - 27.51	15.94	10.0 - 28.0
Water Content (%)	14.0	10.5 - 17.5	10.0	8.2 - 13.0
Relative Saturation (%)	80	60 - 100	60	42 - 82
Sat. Hydraulic Cond. ($m\ s^{-1} \times 10^{-9}$)	20.47	0.36 - 438	0.55	0.0001 - 5.86
Fracture Density (m^{-1})	0.77	0 - 4.33	5.02	2.17 - 10.9

ALTS is located near the extreme western edge of the Pinal Mountains which rise to over 2100 m in elevation. Lying immediately east of Superior, Arizona, is the Apache Leap which forms a 600 m west-facing escarpment that exposes a volcanic zoned ash-flow tuff sheet and an underlying carbonate (Figure 2). ALTS is approximately one km to the east of the escarpment at an approximate elevation of 1200 m. The rocks exposed at the site are the uppermost unit of a sequence of ash-flow tuff sheets, which extend to a depth of approximately 580 m below the site. The tuff is a consolidated deposit of volcanic ash with particle diameters less than 0.4 mm resulting from a turbulent mixture of gas and pyroclastic materials of high temperature about 19 million years ago. The ash-flow deposits at one time covered an area of approximately 1000 km^2 with a maximum thickness of 600 m but have been eroded in some places to about 150 m in thickness (Peterson, 1961).

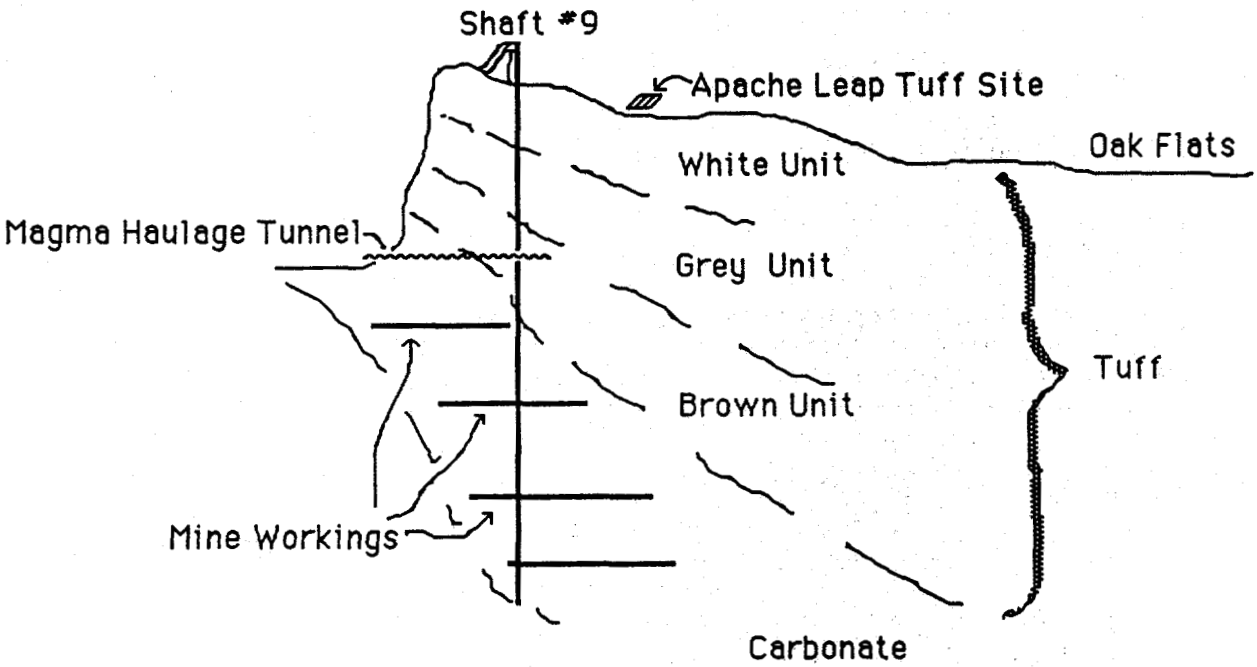

Figure 2: Cross-sectional view of Apache Leap Tuff showing Magma Mine workings, haulage tunnel, Shaft Number 9, Apache Leap Tuff Site, and general geologic structure. Not drawn to scale.

Atmospheric precipitation is recorded near the site and the long-term average is estimated to be approximately 538 mm yr^{-1}. Most of the precipitation occurs during two periods, from mid-July to late-September, and from mid-November to late-March. Summer storms are characterized by high-intensity, short-duration thunderstorms during periods of high temperature and evapotranspiration demand. Winter storms are of longer duration and lower intensity during cooler periods with much lower evapotranspiration demand.

Regional ground-water levels below the site have been substantially modified by dewatering activities at the nearby Magma mine which extends to a below the site. The water levels have been drawn down to levels below the tuff unit. Perched water has been observed at several locations near the site, notably in shallow alluvial aquifers along major washes and from seeps near washes. Noticeable increases in inflows to the main haulage tunnel for the Magma mine are observed within days following streamflow in Queen Creek, which is located approximately 100 m above the haulage tunnel. Observations in mine workings at deeper levels demonstrate increased inflows up to several weeks following streamflow events.

Twelve inclined and three vertical boreholes have been installed at the site in five sets of boreholes (Figure 3). Each set consists of three boreholes drilled in a plane. The inclined boreholes are not of the same length, with the lengths of the boreholes being 15, 30 and 45 m. This design results in the bottom of each borehole in a series lying along the same vertical line. Two inclined borehole sets are parallel to each other and the other two inclined sets are oriented 90° and 180° to the first two sets. A fifth set of boreholes are oriented vertically and penetrate to a depth of 30 m. A plastic cover has been placed over the rock surface to cover an area of approximately 30 x 50 m. The cover is designed to prevent evaporation from the rock to the atmosphere as well as to prevent precipitation from infiltrating into the rock.

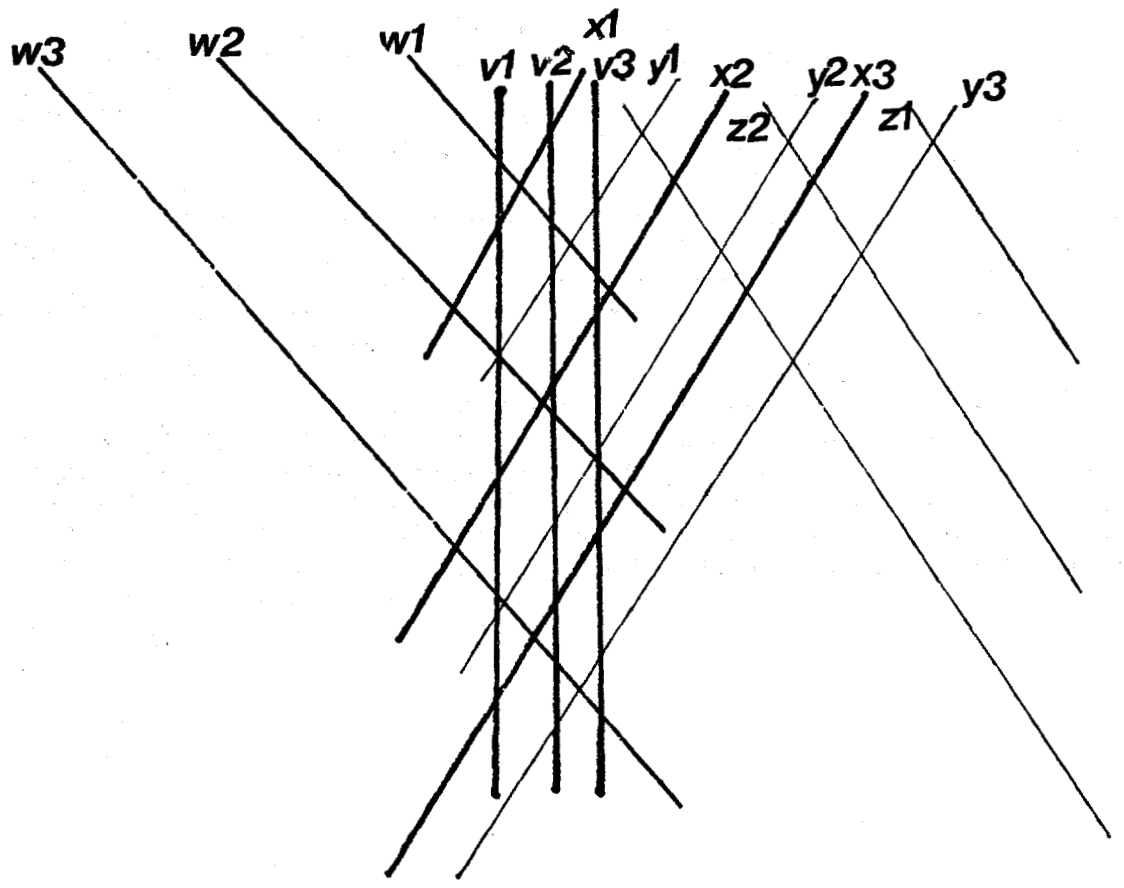

Figure 3: Borehole installations at the Apache Leap Tuff Site.

2. UNSATURATED FLOW AND TRANSPORT CHARACTERIZATION

2.1 Role of Characterization

The evaluation of the suitability of a candidate site for the permanent geologic disposal of HLW requires that an assessment of the performance of the site be performed with respect to activities related to the construction, operation and closure of the HLW facility. An important component of the site performance assessment is the characterization of the site with respect to individual performance parameters. The performance parameters, which are specified in such documents as 10CFR60, include, for example, the pre-emplacement ground water travel time to the accessible environment.

Table 2 presents the site characterization process with respect to hydrogeologic radionuclide transport. An important requirement of the site performance assessment is the characterization of the uncertainties associated with the conceptual models, governing equations and parameters. The uncertainties are used to evaluate the reliability of site performance forecasts. Estimates of parameter uncertainty due to measurement and spatial variability must be determined using field and laboratory tests. The tests are also useful for verifying the validity of the governing equations and identified processes and mechanisms used to construct the conceptual model.

Table 2: Site characterization process definition.

STEP	
1	A conceptual model is developed in which the dominant interstitial, hydraulic, pneumatic, chemical, and thermal mechanisms, processes and interrelationships are determined. All possible components are included initially and processes not relevant to site characterization are removed as characterization progresses.
2	The governing equations and parameters which describe the dominant mechanisms and processes are identified.
3	Representative values of parameters are estimated from laboratory and field testing programs, from natural analog studies, or from geochemical information.
4	Forecasts of site performance with respect to performance parameters are generated using site specific information.
5	Confirmatory experiments are conducted to evaluate the predictive capability of the forecast models. Errors in forecasts are quantified to determine risks associated with forecast uncertainties.

Comparisons of data sets obtained using various techniques spanning a wide range of conditions and implicit assumptions concerning flow processes are an integral part of site characterization. Potential biases may not be resolved without confirmatory data sets from diverse sources, including information from short-term field tests along with geochemical and natural analog information. The inability to resolve potential biases may result in the false acceptance of a site that would not be suitable for long-term HLW isolation.

2.2 Flow and Transport Mechanisms

As can be observed in Table 2 (above), predictive models are required to provide forecasts of repository performance. Predictive models of fluid flow and solute transport through a homogeneous, isotropic, isothermal, unfractured, unsaturated porous medium under conditions of uniform spatial and temporal application of water at the surface are easily constructed using analytic and numerical methods. For most field conditions, especially those in the vicinity of a proposed high-level nuclear waste repository, these fundamental characteristics are not expected to be encountered and the influences of phenomena such as matrix heterogeneities like lenses and layering, fractures, nonisothermal conditions, multiphase and multicomponent transport, and episodic and spatially variable infiltration must be evaluated. In addition, the influences of parameter and process uncertainties are not entirely known with respect to performance assessment. This NRC-funded research program focuses on understanding and defining the relevant processes, assessing the relative importance of each process, and determining effective methods for estimating process parameters related to performance assessment.

While many unsaturated hydraulic conductivity relationships have been experimentally determined for soil materials, few such relationships exist for rock, and data for fractured rock are only now becoming available. The presence of fractures and other forms of macroporosity within rock complicates the estimation and prediction of fluid flow and transport. The heterogeneities introduced by the presence of macropores result in complex moisture characteristic curves. For conditions near and at saturation, corresponding to small matric suctions, the fractures may be saturated, causing rapid flow and transport. For larger matric suctions, the fractures may not contribute significantly to fluid flow, and may even form barriers to the flow of liquid water. Multiphase flow of water within the unsaturated zone is also possible. While an air-filled void may reduce liquid flow, the decrease in liquid flow can be partially offset by increases in vapor diffusion. Movement of water vapor through open fractures may constitute a significant fraction of the total fluid movement under certain conditions. The relative magnitude of vapor versus liquid flow depends on site specific features.

The movement of solutes within unsaturated fractured media may be rapid for saturated fractures within rock of low permeability. Substantial attenuation of solute transport will occur if fluid flow velocities are low and the rock bounding the fractures is permeable allowing diffusion of solutes into the rock matrix. Also, fractures may remain drained at large matric

suctions resulting in lower flow velocities and longer travel times. Processes that would tend to accelerate solute velocities include channeling within fractures as well as zones of saturation lying above lower permeability horizontal structures. Release rates of contaminants will be a function of the flow rate as well as the flow velocity, both of which may increase when saturated fractures are present.

Heat production by HLW will alter the pre-emplacement hydrologic environment. Enhanced vapor transport away from the heat source and subsequent condensation will change fluid and transport properties around the repository. Increases in fluid saturation may result in saturation of fractures, and substantial increases in fracture flow and decreases in travel times. Countercurrent flows in the rock matrix will affect fluid and solute transport near the repository. The redistribution of water in response to a thermal loading may inhibit the release of radionuclides under certain scenarios, while enhancing releases under other scenarios. The evaluation of the likelihood and risks associated with specific scenarios requires that alternate conceptual models be developed and evaluated using field and laboratory data.

For variably saturated geologic materials the flux rate generally decreases as the matric suction of the medium increases. Also, as flux rates decrease travel times generally decrease. Exceptions to these statements are common, especially for heterogeneous materials under conditions of rapidly changing boundary conditions. For a recharge event from the earth's surface through an open fracture within a rock matrix at an initially high matric suction, the fluid pulse may cause transient suctions within the fracture to develop that are substantially different from the matric suction within the rock matrix which bounds the fracture. Over time, pressure heads between the fracture and matrix may equilibrate depending upon the degree of channeling within the rock matrix, as well as the permeability of the fracture walls and the rock matrix.

Travel times and flux rates are also dependent on the geometry of the flow problem. The flow geometry is important in unsaturated media due to the strong relationship between fluid velocity and the size of saturated pores. For a regime where fluid flow is uniformly distributed through the smallest pores, the average fluid velocity will be smaller as compared to an equal flow volume through a few large channels. The correct geometry is also important for model specification, parameter estimation, and flow prediction. While a three dimensional flow equation may be appropriate for an unfractured porous medium, flow through individual fractures will be one- or two-dimensional depending upon whether substantial channeling is present or not (Figure 4).

The scale of observation may also affect the selection of the model used to represent the flow geometry. Combining flow through one dimensional channels into a network of channels may result in the selection of a two dimensional flow model, while combining two dimensional flow through individual fractures into a network of fractures may result in the selection of a three dimensional flow field model. The opposite process of consolidation of flow into a few specific flow paths can also occur. In

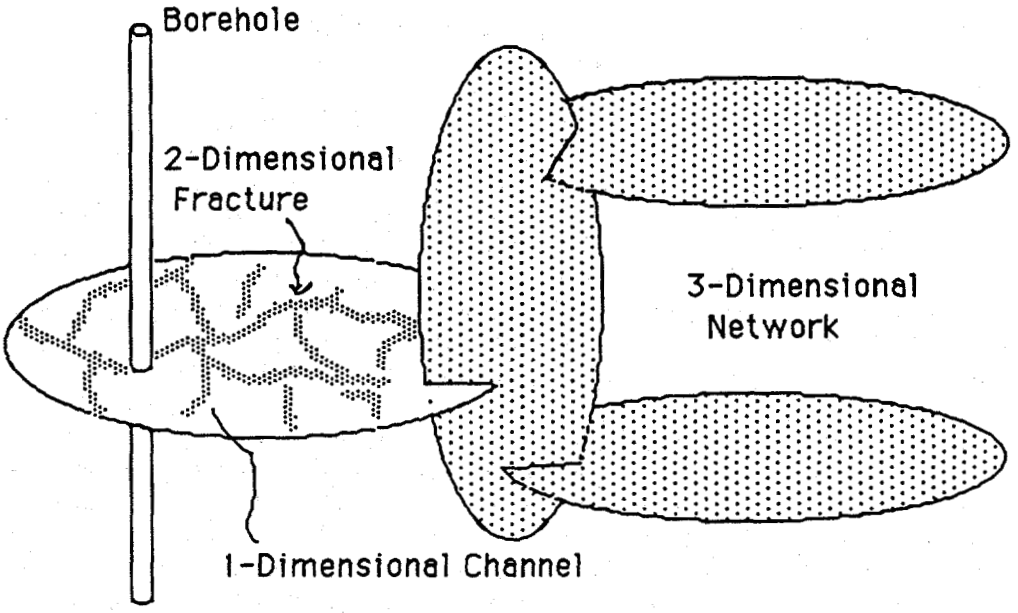

Figure 4: Dimensionality of flow in fractures is variable depending upon the scale of investigation. Flow in channels within fractures may be one-dimensional, but two-dimensional when considering an interconnected network of channels within a discrete fracture, as shown. Flow through a large network of fractures may be characterized as three-dimensional if the fractures are sufficiently interconnected.

order to evaluate these issues, Rasmussen and Evans (1989) address the importance of fracture geometry and scale effects on travel time and flux rates in unsaturated fractured rock.

2.3 Characterization of Fracture-Matrix Systems

The application of forecast models for the purpose of predicting flow and transport through geologic media is a necessary and important component of site characterization activities. The forecast models are either analytic or numeric, and require that the important relevant processes and data be incorporated. Of primary concern in this section is the specification of fluid flow through unsaturated fractured rock with respect to the presence of multiple porosities, i.e., fracture and matrix porosity, as well as the presence of multi-dimensional flow through the various porosities.

Various flow routes are possible for water and entrained solutes in unsaturated media. For conditions of large matric suctions, corresponding to low relative saturations, the assumption that fractures will not contribute to fluid flow results in a regime where all flow occurs through the rock matrix. This idealized representation of flow through heterogeneous materials ignores interactions between fractures and the rock matrix. An alternate extreme flow scenario is to assume that infiltration pulses from the earth's surface are not attenuated by the rock matrix as the water travels through channels within discrete fractures. In this scenario, all flow occurs within fractures with little flow through the rock matrix. Another scenario assumes that fluid flow will occur through both the rock matrix and a network of discrete fractures embedded within the matrix in response to local variations in geometric and hydraulic properties. Yeh et al. (1988), Rasmussen (1987) and Rasmussen and Evans (1989) have investigated coupled fracture-matrix flow scenarios in unsaturated fractured rock.

Incorporating flow through both a permeable matrix and fracture network within a single model has been the goal of numerous investigations. Various formulations have been developed to simultaneously solve flow through the two porosities, with each formulation having various advantages and disadvantages. The various formulations, described below and presented in Table 3, include the equivalent porous medium, dual porosity, discrete fracture, percolation, and stochastic representation methods.

The first method described in Table 3 is to combine both porosities into a single porous medium model using effective parameters. This equivalent porous medium (EPM) formulation is accurate and very efficient for a flow regime that is dominated by a single porosity and when the test conditions for which the effective parameters were estimated match the conditions which will be simulated.

A second technique has been to use a dual porosity (DP) formulation with two flow models simultaneously solving flow through each medium after allowing for linkages between the two media. The DP formulation is still efficient, but may not accurately reproduce the fracture network geometry if a regular grid is employed to simulate fracture flow.

Table 3: Alternate conceptual formulations of fluid flow

	Formulation	Attributes
EPM	Equivalent Porous Medium	Single continuum with effective parameters used to combine fracture and matrix properties
DP	Dual Porosity	Two continua, one for fractures and second for matrix, with linkages between continua.
DFN	Discrete Fracture Network	Discontinuous fracture network constructed from geometric information about fractures.
PN	Percolation Network	Regular nodal network connected by bonds with prescribed probabilities.
SR	Stochastic Representation	Perturbation analysis of influence of small variations of material properties.

The discrete fracture network (DFN) technique takes advantage of available geologic information about fracture orientations, densities and spatial extent, and hydraulic properties to build a network of interconnected fractures that can be used to simulate flow under a wide range of initial and boundary conditions. The shortcomings of this technique are uncertainties related to fracture network geometries, and the intensive computational effort required.

The use of percolation networks (PN) to represent flow through multiple porosities allows the incorporation of information about local variations in pore and fracture interconnectivity to be used to generate macroscopic effective parameters. Required additional microscopic parameter information such as pore shape and tortuosity are often not available and are potential drawbacks to the application of this technique to macroscopic flow problems.

A final technique uses a stochastic representation (SR) of the flow equations to incorporate spatial heterogeneities in material properties. While limited to applications where the perturbation from average conditions is small, the SR formulation provides analytic results that are useful for model calibration and validation, as well as investigating the effects of scale on effective parameters.

2.4 Characterization of Coupled Liquid-Vapor Flow and Transport

While pre-emplacement ground water travel times from the repository horizon to a fixed boundary may indicate the ability of the geologic setting to restrict the movement of solutes, the travel time calculated by this method may have little relevance for predicting solute transport from the repository once the wastes are in place. The thermal effects of the repository will result in substantial modification of the hydrology, especially near the repository. Effects are not limited to the immediate region around the repository, but may also extend to the ground surface. Significant drying of the rock near the repository will result in a similar volume of condensate somewhere else. The increased saturation in the condensing region may result in zones of positive fluid pressures and induce fracture flows near the repository.

Several computer programs capable of simulating coupled liquid and vapor flow were studied and compared. These codes include NORIA, PETROS, TOUGH, and TRACER3D, described below. The ability of the four computer programs to assess liquid-vapor flow under a variety of hypothetical site conditions and spent fuel leaching scenarios was compared. These scenarios include one-dimensional horizontal infiltration, one-dimensional heat transport, radial heat transport, radial boiling front, heat pipe, two-dimensional infiltration, and a two-phase flow condition. All the codes reviewed are extremely difficult to use. While the codes are capable of simulating vapor phase flow and transport, none of them are designed to simulate the complete transport behavior of radionuclides. Furthermore, all the computer programs seemed to have some difficulty with evaporation and condensation problems. However, the TOUGH computer code seems to perform relatively better in the problems examined.

NORIA (Bixler, 1985) is designed to simulate liquid, vapor, air, and energy transport due to pressure, density and temperature gradients in variably saturated porous and fractured media. It includes many mechanisms that may exist in water, vapor, and air flow systems, such as binary diffusion of vapor and air, Knudsen diffusion of vapor and air, thermo-diffusion of vapor and air, conduction and convection of sensible heat, evaporation and condensation, and capillary pressure at the interface of water, vapor, air, and solid. Four nonlinear partial differential equations are used in NORIA to describe the flow of water, vapor, air, and energy. These equations consist of a water-pressure equation, a vapor partial pressure equation, and a heat equation. Using the Galerkin finite-element method, these partial differential equations are then transformed to a system of nonlinear algebraic equations which is solved using the Newton-Raphson iteration scheme.

PETROS (Hadley, 1985) is another computer model designed to simulate liquid, vapor, air, and energy transport in partially or fully saturated porous and fractured media. The conceptual formulation of the governing partial differential equations for the flow and transport processes in PETROS is identical to that in NORIA. However, PETROS considers only one-dimensional, radial, or spherical flow systems. PETROS solves three mass conservation equations and a heat conservation equation just as NORIA.

However, the liquid conservation equation in PETROS is formulated with respect to saturation rather than pressure as in NORIA. The characteristic curves and the thermal conductivity as a function of saturation and temperature are supplied to PETROS through user-written function subprograms. Other parameters such as diffusion coefficients, water viscosity, saturation vapor pressure of water, and thermal conductivity are supplied internally in the code as function subprograms. Constants such as gas viscosity, specific heats, and water density can either be set at default values or supplied by the user. The user can also choose between equilibrium and non-equilibrium vapor-pressure models. The governing partial differential equations are approximated by a set of algebraic equations using a fully implicit finite difference scheme. Because the flow system is limited to one-dimensional problems, the saturation and temperature equations are solved with a tridiagonal algorithm. A block tridiagonal algorithm is employed to solve the strongly coupled vapor and air pressure equations.

TOUGH (Pruess, 1987) simulates fluid flow in both liquid and gaseous phases due to pressure, viscous and gravity forces in accordance with Darcy's law, and with interference between phases as represented by relative permeability functions. Binary diffusion in the gas phase is also considered. Not considered are Knudsen diffusion, and hysteresis in either capillary pressure or relative permeability. Thermophysical properties of liquid water and vapor are obtained from steam table equations. Air is treated as an ideal gas, and Dalton's law is assumed for air and vapor mixtures. Air dissolution in water is described by Henry's law, but the temperature dependence of Henry's constant is neglected. Heat transport is modeled along with binary diffusion, which incorporates both sensible and latent heat transfer. The governing equations in TOUGH are applicable to one-, two-, and three-dimensional anisotropic porous and fractured media. TOUGH does not perform stress calculations for the solid skeleton, but does allow for porosity changes in response to changes in pore pressure and temperature using compressibility and expansivity coefficients, respectively. The governing equations for air, water, and heat flow in TOUGH are approximated by a general integrated finite-difference method. The resulting nonlinear difference equations are solved by the Newton- Raphson technique and the Harwell matrix solver that can reduce the computer memory requirement for the code.

TRACER3D was developed by B.J. Travis (Oster, 1982) at Los Alamos National Laboratory to model time-dependent two phase flow under isothermal conditions and chemical species transport in a three-dimensional, deformable, heterogeneous, reactive porous and fractured medium. The equations that comprise the TRACER3D model are the mass conservation equations for liquid, gas, and chemical species, a reduced form of the momentum equations, an equation of state, and several constitutive relations. The governing partial differential equations are approximated by using a fully implicit, block centered, backward time finite difference scheme. Equations describing flow of liquid and gas are coupled and solved simultaneously for the pressures in each phase. The solution technique used in the model is a Gauss-Seidel successive over-relaxation method.

3. UNSATURATED FLOW AND TRANSPORT PARAMETERS

In order to parameterize hydrologic flow and transport, the flow domain is divided into two dominant porosity components consisting of a matrix and a fracture porosity. Laboratory core segments obtained from ALTS are used to acquire information about matrix properties at 105 locations in nine of the test boreholes (Figures 5 and 6). Interstitial properties include bulk and grain density, effective porosity, pore surface area, and pore size distribution. Hydraulic matrix properties include saturated and unsaturated hydraulic conductivity, as well as the moisture characteristic curve for each core segment. Pneumatic properties include the oven-dry and unsaturated air-phase permeability, and the Klinkenberg slip-flow coefficient which can be used to estimate the Knudsen diffusion coefficient. Thermal properties include the moisture dependent thermal conductivity and rock heat capacity.

Vogt (1988) presents data that provides characterization data with respect to the distribution, size and interconnectedness of pores in samples from unsaturated rock matrix at ALTS. This study examines the use of mercury porosimetry in determining porosity, pore-size distribution and pore surface area of unsaturated, slightly welded to densely welded tuff at ALTS. 121 samples of tuff were subjected to mercury intrusion pressures to 200 Mpa. A bimodal pore-size distribution exists for all samples of slightly welded tuff with the larger pore size class mode diameter averaging 2.91 μm and the lower pore size class mode diameter averaging 0.07 μm. Interconnected porosity, pore surface area and bulk density averaged 14.62%, 3.46 $m^2\ g^{-1}$ and 2.13 $Mg\ m^{-3}$, respectively. On average, 52.73% of the porosity was accounted for by the large pore size class, while 96.28% of the pore surface area was accounted for by the small pore size class. Samples of densely welded tuff exhibited a unimodal pore-size distribution with an average mode diameter of 0.035 μm.

In a separate study, Goering (1988) used gamma ray geotomography to measure the dry bulk density and porosity distributions in two cores of ALTS tuff. The cores were then subjected to a point or non-point source of water, and water movement through the cores was observed using tomography. Three numerical methods, the Algebraic Reconstruction Technique (ART), modified ART, and Singular Value Decomposition (SVD) were used to reconstruct the tomographs. The SVD method was found to be superior for the simple tomographs of this study. Several tomographic models were used to determine the maximum image resolution from a given set of data. The effects of increasing the number of gamma ray measurements on resolution were also studied. Finally, the tomographs were compared with laboratory measurements for validation. The tomographically predicted dry bulk density distributions were similar to the measured dry bulk density distributions within each core. However, the percent saturation tomographs were found to be inaccurate when water was rapidly moving through the cores because of the considerable time required to obtain the numerous gamma ray attenuation measurements. The method provides good spatial resolution maps at low flow rates, however.

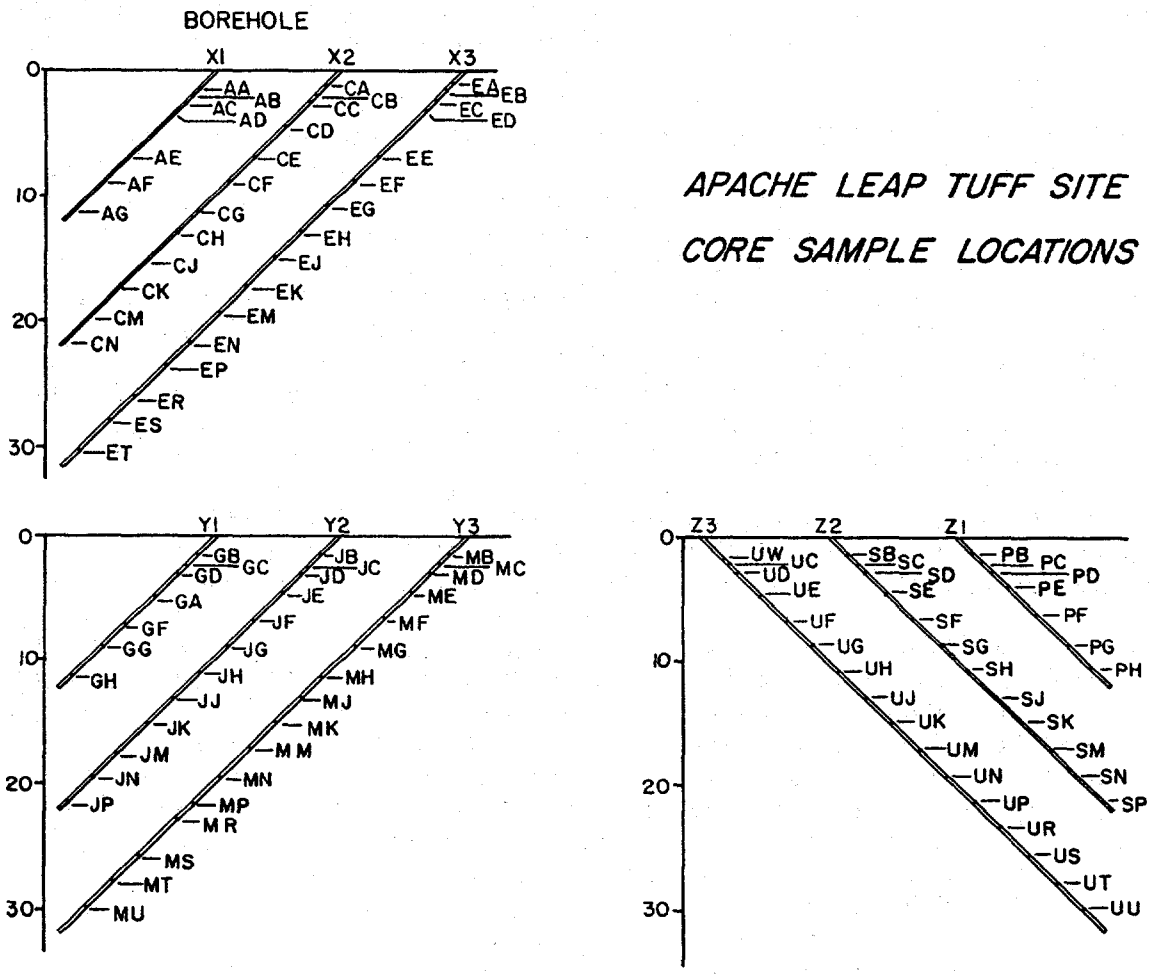

Figure 5: Locations of samples collected from cores at three meter intervals. Field tests and measurements are centered at the same locations.

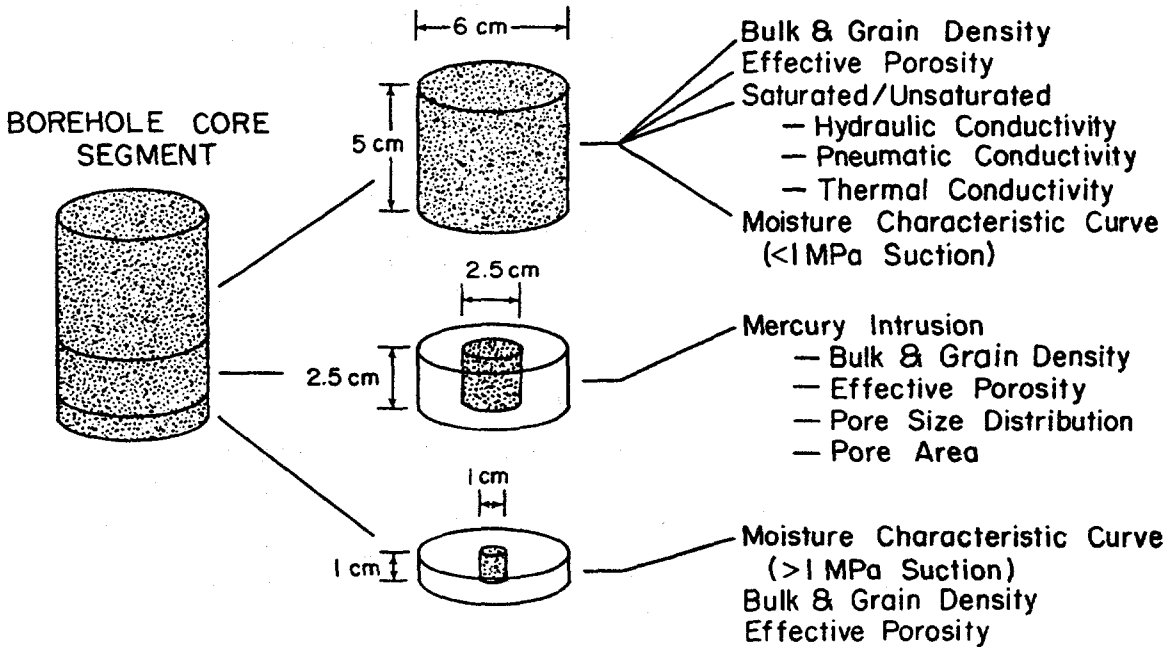

Figure 6: Dimensions and uses of segments cut from cores obtained at the Apache Leap Tuff Site.

Oriented core segments can also be used to obtain fracture density and orientation information. Field parameter estimates incorporate both fracture and matrix properties. Field hydraulic conductivity, air permeability, and thermal diffusivity are available for interpretation and comparison with laboratory data sets. Both single hole injection tests, as well as cross hole data tests provide information useful for evaluating the relative importance of fracture and matrix flow as a function of scale and ambient matric suction.

Tidwell et al. (1988) describe a method which is used to estimate the equivalent saturated hydraulic conductivity and its associated spatial distribution in fractured rock situated in the vadose zone. Conductivity is estimated in part from outflow rates, induced by a nearly constant hydraulic head, monitored over three meter intervals in boreholes which are oriented in a manner so as to intersect the major fracture sets of a field site. Outflow rates are monitored using a volumetric flowmeter while borehole intervals are isolated with a single inflatable packer. Upon collection of the field data, hydraulic conductivity values are estimated by means of two analytical solutions. The solutions are adapted to meet the special conditions posed by variable borehole orientations and multiple test intervals from existing solutions associated with borehole permeability tests. The developed methodology is subsequently utilized to determine the saturated hydraulic conductivity and associated spatial variability in fractured rock at the Apache Leap Tuff Site.

3.1 Interstitial Characterization Parameters

Characterization of the rock interstitial properties is performed using oriented cores obtained during borehole drilling. Properties of the rock matrix were obtained using a regular sampling system, while fracture parameters were obtained by performing an inventory of all apparent fissures observed in the cores.

Matrix Interstitial Properties

Interstitial properties of the rock matrix are obtained at 105 sample locations using rock core samples of the three segment sizes described above. The measured interstitial properties of the core segments include the bulk density, skeletal density, effective porosity, and pore area. The pore area is available only for the medium segment, while the other properties are reported for the three segment sizes.

The bulk density is the dry rock mass per unit volume, determined for the large and small segments by oven drying the rock sample at 105°C until a constant mass is obtained, weighing the rock segment to determine its mass, and then measuring the dimensions of the segment for computing its volume. The bulk density of the medium segment was determined using the mercury intrusion method, which takes advantage of the nonwetting property of mercury. A rock segment with a known dry mass is placed inside a chamber of known volume and the mass of mercury needed to fill the chamber is measured. The volume of the rock segment is calculated by subtracting the volume of intruded mercury from the volume of the chamber.

Table 4 summarizes bulk density data for all 105 samples and for all three segments. Only moderate dispersion about the mean is evident, equal to approximately three percent of the mean value of 2.10 Mg m^{-3} for the large segment. The range of values shown in Table 4 varies with the segment size, and is between 1.75 and 2.25 Mg m^{-3}. A substantial skew in the data is not evident, as noted by the similarity between the mean and median values in Table 4. The bulk density data for the small segment is generally less than for the other segments.

Table 4: Summary of bulk density values obtained from core segments at ALTS.

	BULK DENSITY (Mg m^{-3})		
	small	medium	large
Mean	1.99	2.13	2.10
C.V., %	4	3	3
Minimum	1.75	1.94	1.86
Median	2.00	2.14	2.12
Maximum	2.17	2.25	2.20

The effective porosity of the rock matrix is the volume of interconnected voids per unit volume of rock, exclusive of any isolated pores or large openings, such as fractures and sizable solution openings. The effective porosity is measured for the small and large segments by determining the difference in mass between a saturated segment and an oven-dried segment. The difference in mass is divided by the density of water and the volume of the segment. For the medium segments, mercury is forced under pressure into the segment. The effective porosity is calculated by measuring the volume of mercury intruded into the sample and dividing by the volume of the sample and the density of mercury. The mercury intrusion method will underestimate the effective porosity because the volume of mercury intruded at the maximum pressure is less than the volume of water intruded due to the nonwetting property of mercury. Using capillary theory, rock pores and crevices with curvatures corresponding to a diameter of less than approximately 6 nm will not be intruded with mercury for the experimental equipment used.

Table 5 presents a summary of effective porosity data for all three segments at all 105 sample locations. The mean effective porosity varies from 14.62 to 17.50 percent, depending upon the method of analysis, with the mercury intrusion method consistently underestimating the porosity due to the non-wetting property of mercury. The variability using both methods is greater than the estimated bulk density, with the coefficient of variation ranging from 13 to 26 percent of the mean value. The range is also large, 11 to 25 percent for the small, 9 to 48 percent for the medium segment, and 14 to 28 percent for the large segment.

Table 5: Summary of effective porosity values obtained from core segments at ALTS.

	EFFECTIVE POROSITY (%)		
	small	medium	large
Mean	17.15	14.62	17.54
C.V., %	16	26	13
Minimum	11.02	9.18	14.30
Median	16.52	14.31	17.21
Maximum	24.73	47.58	27.51

The pore surface area is the interfacial area between the wetting fluid and the rock matrix, obtained using the mercury intrusion method. The medium sized segment is placed inside a penetrometer, which is then evacuated and filled with mercury. The volume of mercury added is measured gravimetrically and the volume of the sample is determined by subtracting the volume of mercury from the volume of the penetrometer. Mercury is then intruded under pressures up to 175 MPa in predetermined increments. The volume of intruded mercury at each pressure increment is determined by measuring the change in electrical capacitance of mercury in a fill tube. The applied pressure is used to determine a pore diameter using capillary theory. The surface area for each increment of intruded volume is calculated by noting that the total work expended per unit area of surface covered during a pressure step is related to the surface tension. Table 6 presents summary pore surface area statistics. The data indicate that the mean pore area is 3.466 $m^2\ g^{-1}$ with a coefficient of variation of 65 percent, which is large relative to other matrix interstitial parameters, and ranges from 1.96 to 16.51 $m^2\ g^{-1}$.

Table 6: Summary of pore area values obtained from medium core segments at ALTS.

	PORE AREA ($m^2\ g^{-1}$)
Mean	3.466
C.V., %	65
Minimum	1.960
Median	3.009
Maximum	16.510

The distribution of pore sizes can be estimated using the mercury intrusion technique described in the previous section. If a uniform contact angle and surface tension is assumed between the mercury and the rock surface, then an equivalent pore diameter can be estimated using capillary theory. As part of the mercury intrusion procedure, the cumulative intrusion volume is measured for each pressure increment, which can then be used to construct a distribution of intrusion volume as a function of equivalent pore diameter. Table 7 summarizes cumulative intrusion volumes.

Fracture Interstitial Properties

Interstitial properties of fractures are obtained primarily from oriented cores extracted at the time of borehole construction. Fracture locations are identified by position with respect to an arbitrary coordinate system which is oriented to be coincident with the borehole orientations. The data indicate that fractures are located throughout the length of the boreholes, with some intervals having more fractures than others. Observed fracture density data are presented as Table 8. From ALTS data it can be observed that fracture density variation is high, ranging from a density of no fractures per three meter interval to a maximum of 4.3 fractures per meter, which is noted at two locations. The distribution has the appearance of an exponential distribution, which is consistent with a Poisson process for fracture locations. Mean fracture spacing is the reciprocal of fracture density.

Mathematical, graphical and mechanical methods were used for correcting the apparent dips of fractures in the oriented drill cores taken from inclined boreholes. A graphical technique using a stereonet was used to verify the results. The procedure consists of assuming that the borehole is vertical when the observed angles are measured for a fracture plane intersecting the core. The borehole is then tilted into its inclined position and the resulting true dip and strike are calculated.

The absolute orientation of fracture traces in the drill core are determined by measurement of the angle between the fracture plane and the core axis and the angle between the major axis of the elliptical trace of the fracture plane and a line scribed on the drill core, measured on the circumference of the core. The apparent angles of the fracture plane were measured in the laboratory using a goniometer. The data indicate the presence of many north-south trending fractures which dip steeply to the west as well as a few randomly oriented fractures. This is not entirely consistent with surface fracture traces, which also include steeply dipping, east-west trending fractures. This additional fracture set is not evident in the borehole cores either due to the positioning of the boreholes parallel to the fracture set, or due to the lack of such fractures in the immediate vicinity of the boreholes.

Table 7: Summary of cumulative intrusion volume as a function of equivalent pore diameter.

	CUMULATIVE INTRUSION VOLUME (m^3 m^{-3})							
	- - - - Equivalent Mean Pore Diameter (μm) - - - - -							
	13.8	9.19	7.64	6.30	5.08	4.06	3.27	2.61
Mean	0.0003	0.0005	0.0011	0.0024	0.0060	0.0125	0.0213	0.0308
C.V., %	869	601	317	173	108	79	58	44
Minimum	0.0000	0.0000	0.0000	0.0000	0.0000	0.0000	0.0000	0.0000
Median	0.0000	0.0002	0.0004	0.0009	0.0032	0.0106	0.0205	0.0310
Maximum	0.0295	0.0310	0.0318	0.0329	0.0346	0.0447	0.0580	0.0684
	- - - - Equivalent Mean Pore Diameter (μm) - - - - -							
	2.07	1.65	1.30	1.03	0.802	0.627	0.494	0.385
Mean	0.0410	0.0487	0.0544	0.0590	0.0631	0.0666	0.0696	0.0726
C.V., %	36	36	35	35	34	33	32	32
Minimum	0.0000	0.0000	0.0000	0.0000	0.0000	0.0006	0.0019	0.0029
Median	0.0426	0.0494	0.0560	0.0608	0.0643	0.0672	0.0714	0.0747
Maximum	0.0762	0.0907	0.1067	0.1154	0.1221	0.1273	0.1319	0.1356
	- - - - Equivalent Mean Pore Diameter (μm) - - - - -							
	0.302	0.237	0.187	0.146	0.115	0.0896	0.0700	0.0548
Mean	0.0756	0.0787	0.0819	0.0859	0.0907	0.0969	0.1042	0.1116
C.V., %	31	30	29	26	24	22	21	20
Minimum	0.0043	0.0058	0.0076	0.0107	0.0149	0.0196	0.0239	0.0287
Median	0.0774	0.0807	0.0829	0.0861	0.0901	0.0975	0.1042	0.1110
Maximum	0.1387	0.1421	0.1456	0.1489	0.1527	0.1568	0.1614	0.1662
	- - - - Equivalent Mean Pore Diameter (μm) - - - - -							
	0.0429	0.0336	0.0262	0.0205	0.0160	0.0125	0.0098	0.0077
Mean	0.1182	0.1237	0.1284	0.1327	0.1369	0.1397	0.1417	0.1428
C.V., %	19	19	17	16	15	15	14	14
Minimum	0.0345	0.0398	0.0535	0.0759	0.0871	0.0888	0.0901	0.0911
Median	0.1189	0.1250	0.1294	0.1330	0.1358	0.1389	0.1410	0.1423
Maximum	0.1710	0.1749	0.1776	0.1795	0.2023	0.2064	0.2092	0.2113

Table 8: Summary of ALTS borehole fracture density and orientation.

	FRACTURE DENSITY (m^{-1})	FRACTURE ORIENTATION Strike (°)	Dip (°)
Mean	0.77	214.4	64.5
C.V., %	108	56	37
Minimum	0.00	3.	1.
Median	0.67	109.	55.
Maximum	4.33	359.	89.

3.2 Hydraulic Characterization Parameters

Hydraulic properties reported here are divided into matrix and combined fracture-matric properties. Matrix properties are obtained from the large core segments, as described above, while combined fracture-matrix properties are derived from field testing procedures. The measured hydraulic properties of the rock matrix include the saturated hydraulic conductivity, moisture characteristic curve, and the unsaturated hydraulic conductivity curve. Field water content data are used to estimate field matric potentials using laboratory moisture characteristic curves. In addition to the rock matrix characteristics, field and laboratory data sets are used to characterize the fracture hydraulic properties, as well as coupled fracture-matrix properties when the two can not be differentiated.

Matrix Hydraulic Properties

Laboratory analysis of oriented borehole core segments are used to determine the hydraulic properties of the rock matrix. Because the rock segments were selected specifically excluding fractured intervals, the analyses are only appropriate for characterizing the rock matrix. Addressed in this section are the saturated flow properties, as well as the effect of variable saturation on the hydraulic properties.

The moisture characteristic curve relates the water content or relative saturation of a rock sample to the matric suction of the water in the sample. The drainage portion of the moisture characteristic curve is obtained for the wet region (i.e., matric suctions less than 500 kPa) using the large core segments in conjunction with a pressure extraction vessel, while the data for the dry region (i.e., matric suctions greater than 500 kPa) are obtained using the small core segments in conjunction with a thermocouple psychrometer and a sample changer.

For matric suctions less than or equal to 500 kPa, a pressure plate extractor is used to control the matric suction within a core segment. The procedure consists of saturating a large rock segment, placing the segment on a pressure plate (using a silica paste to establish a good hydraulic connection between the plate and the segment), sealing the pressure plate within the pressure vessel, and applying a desired matric suction using

nitrogen gas to pressurize the vessel. Once the sample has reached equilibrium, the pressure is released, the vessel is opened, the sample is removed and the moisture content of the sample is determined gravimetrically. The sample is then returned to the pressure plate and a greater pressure is applied. Pressures of 10, 25, 50, 100, 300 and 500 kPa were applied to the cores and corresponding sample water contents were determined.

For matric suctions greater than 500 kPa, a thermocouple psychrometer is used in conjunction with a sample changer chamber. The procedure consists of saturating a small rock segment, placing the segment on a precision balance and drying until the desired relative saturation is achieved, transferring the segment to a chamber in the sample changer, and allowing the matric suction within the segment to equilibrate. Once the suction has stabilized within the chamber, the wet bulb depression of the atmosphere surrounding the rock segment is determined, along with the ambient temperature. From these two measurements the fluid potential within the chamber is determined. The sample is then dried to the next desired relative saturation. Relative saturations from 70 to 10 percent in 10 percent increments are used. Table 9 presents summaries for pressure extractor and thermocouple psychrometer results in tabular form. The data presented here indicate that the saturation of the matrix at a specified matric suction is highly variable, with increasing variation as the suction increases.

Table 9: Summary of laboratory moisture characteristic curve values obtained from ALTS core segments.

	RELATIVE SATURATION (%)					
	Suction (kPa)					
	10	25	50	100	300	500
Mean	95.54	90.54	83.91	70.20	55.90	48.91
C.V., %	4.7	7.6	11.3	12.1	12.9	14.4
Minimum	76.03	70.10	59.05	48.82	38.23	32.71
Median	96.87	92.76	84.93	70.08	56.86	49.18
Maximum	101.21	99.10	97.57	89.07	75.06	69.71

	Suction (kPa)				
	1,000	5,000	10,000	50,000	100,000
Mean	47.5	40.0	22.2	20.8	12.8
C.V., %	19.4	21.3	15.6	26.3	20.3
Minimum	30.	20.	18.	9.	9.
Median	48.	40.	21.	20.	13.
Maximum	68.	60.	31.	34.	16.

The hydraulic conductivity is a coefficient which relates the hydraulic head gradient to fluid flux according to Darcy's law. To determine the saturated hydraulic conductivity, the core segment is saturated under a vacuum, and then the fluid flux is determined by dividing the volumetric flow rate as measured by a flow meter by the cross sectional area. For one-dimensional steady flow the hydraulic gradient is determined by dividing the total head drop across the sample by the length of the sample. The total head drop is calculated by noting that the total head is the sum of the pressure and elevation heads.

The procedure employed to measure the saturated hydraulic conductivity from rock core segments uses the large segments in conjunction with a permeameter. The permeameter consists of an inflatable packer which is used to seal the annulus between the rock segment and an outer brass collar. Covers are placed over each end of the permeameter and water is introduced under pressure at the upper surface of the rock segment. Outflow from the lower surface is collected and measured using a flow meter. Prior to performing the measurement the rock core is saturated using sterile, 0.001 M $CaSO_4$ solutions.

Table 10 presents summaries of saturated (i.e., a matric suction of 0) and unsaturated hydraulic conductivity for all sample locations. The saturated hydraulic conductivity values vary substantially, over three orders of magnitude, from 0.4 to over 400 x 10^{-9} m s^{-1}, with a mean value of approximately 20 x 10^{-9} m s^{-1}. The distribution of the values appears lognormal with an extended tail toward higher values.

Table 10: Summary of hydraulic conductivity values obtained from 105 large ALTS core segments.

	HYDRAULIC CONDUCTIVITY (m s^{-1} x 10^{-9})				
	Suction (kPa)				
	0	10	25	50	100
Mean	21.31	3.346	1.475	0.908	0.364
C.V., %	301	105	156	115	112
Minimum	0.69	0.126	0.110	0.002	0.005
Median	4.24	2.610	0.556	0.498	0.235
Maximum	438.28	25.750	14.588	5.041	2.541

The hydraulic conductivity of a rock or soil sample is lower at higher matric suctions, or, equivalently at lower water contents. The outflow technique is used to determine the unsaturated hydraulic conductivity of the 105 large core segments. The segments are saturated under a vacuum and then placed inside a Tempe pressure cell. A pressure increment is applied and the rate of outflow from the pressure cell is monitored using a small capacity pipette in conjunction with an air bubble which is injected through a septum at the upstream end of the pipette. A recirculation pump is occasionally used to remove accumulated air from the bottom of the porous plate. A burette is used to collect and measure the cumulative outflow from the plate. The unsaturated hydraulic conductivity is determined using an analytic solution for the outflow method when the hydraulic diffusivity is a constant over each pressure increment. For the samples and pressure increments employed in this analysis, however, the hydraulic diffusivity can not be assumed constant. Instead, an exponentially decreasing hydraulic conductivity is assumed over each pressure step. Using the saturated hydraulic conductivity at zero pressure to begin the procedure, the above equation provides stepwise estimates of the unsaturated hydraulic conductivity. Lacking an analytic solution for the outflow method using this technique, a nonlinear least squares finite element program is used to estimate the unsaturated hydraulic conductivity at each pressure step. Table 10 (above) provides summaries for the unsaturated hydraulic conductivity data.

Field Hydraulic Properties

Field tests of hydraulic conductivity and water content are important for comparison with laboratory data as well as for providing information about the ambient moisture regime at the site of interest. While field hydraulic tests cannot provide data about unsaturated hydraulic properties, they can be used to determine fracture hydraulic properties which are unavailable from core segments. Also, estimates of field water contents can be used to infer the ambient matric suction, and other unsaturated matrix properties.

Hydraulic tests in fractured rock with substantial matrix hydraulic conductivity are difficult to interpret due to the possibility for flow to occur in both the fractures and the matrix. The methodology described here assumes that an effective hydraulic conductivity exists which accounts for saturated liquid flow through both pathways. The equivalent saturated hydraulic conductivities of the fractures intersecting each three-meter borehole interval were determined using a modified falling-head borehole permeability test. The test yields the equivalent conductivity for both the matrix and the fractures.

The method for obtaining the equivalent conductivity involves maintaining a constant water level near the top of a borehole until a constant injection rate is established (Tidwell et al., 1988). A short packer with a tube through it and extending to the surface is lowered to a selected depth in the borehole. The tube extending to the surface is connected to one of three falling-head flow meters calibrated for different flow ranges. When the packer is inflated and the head above and below the packer are maintained equal, the meter measures the injection rate for the length of bore-

hole below the packer. The packer is then lowered 3 m and a similar measurement is made. The difference in measured flow rates is the injection rate for the 3-m borehole segment.

The injection rate is converted to equivalent hydraulic conductivity using three alternate mathematical solution, described in Tidwell (1988). The first solution is a modification of the Glover equation to incorporate inclined boreholes. The second solution is a modification of the Philip equation to again account for the sloping borehole and the packer contained flow. The third solution is the Dachler method. The calculated hydraulic conductivities of the rock surrounding the boreholes using the three methods are summarized in Table 11. Because no particular method is assumed to be a better estimator of the hydraulic conductivity, the modified Glover method is used in subsequent analyses. Like the matrix hydraulic conductivity data, the field data demonstrate a high variability, ranging over five orders of magnitude. The data indicate a high degree of skewness toward the higher values, with two intervals in particular accounting for extreme rates of flow.

Table 11: Summary of field determined outflow rates and saturated hydraulic conductivity values at ALTS.

	INJECTION RATE ($m^3\ s^{-1} \times 10^{-6}$)	HYDRAULIC CONDUCTIVITY ($m\ s^{-1} \times 10^{-9}$)		
		Philip	Glover	Dachler
Mean	26.349	59.42	29.10	30.20
C.V., %	612	729	729	662
Minimum	0.016	0.48	0.27	0.41
Median	0.633	11.63	5.64	10.33
Maximum	1232.	39224.	19126.	17900.

3.3 Pneumatic Characterization Parameters

Air flow through the unsaturated zone can result from pressure and density gradients induced by atmospheric driving forces or subsurface heat generation. The induced air flow can affect subsurface moisture contents and, hence liquid redistribution, by transporting water vapor through air filled porosity. Also, equilibrium of matric potentials between isolated liquid phases can be attained as a result of water transport as vapor. Another important use of air flow monitoring is the assessment of the potential for water transport. The concept of using air as a surrogate test fluid is attractive in that no liquids are introduced which may possibly contaminate subsurface geochemical processes. To evaluate rates and pathways for air flow in the unsaturated zone, methods for estimating the moisture dependent pneumatic permeability of the rock matrix and fracture system are presented here.

Matrix Pneumatic Permeability

The pneumatic permeability for both oven-dried and partially saturated large rock core segments is obtained by employing the permeameter used in the saturated hydraulic conductivity procedure (Rasmussen et al., 1990). A core segment is brought to a desired potential by either drying the segment in a drying oven or by allowing the sample to equilibrate within a pressure extraction vessel. Once a prescribed suction is achieved, the core sample is placed inside the permeameter with the packer inflated to prevent bypassing of air around the outside of the core. A known pressure gradient is applied longitudinally across the core segment and the air flow volume is measured using a calibrated flow meter. The pneumatic permeability at each suction is determined using the measured air flow rate, cross sectional area and core segment length. Because air is compressible, the ideal gas law is employed with the assumption of isothermal flow.

Table 12 summarizes the test results and demonstrates the large variability between samples. The variability is highly skewed, as evidenced by the differences between the mean and median values for all applied suctions. The measured air permeability of an oven-dried sample is usually similar to the measured water permeability. However, for the tuff cores the estimates may not be similar due to slip flow along the walls of pores. The importance of the Klinkenberg phenomenon, as it is commonly called, can be evaluated by comparing the computed air permeability for oven-dried cores with the computed water permeability for completely saturated cores. The two values should be a function of the ambient air pressure used to conduct the air permeability test, as well as the mean free path of the gas molecules and the pore diameter. The effect can be quantified using a Klinkenberg slip-flow coefficient. The coefficient is important because the Knudsen diffusion coefficient can be derived from it.

Table 12: Summary of laboratory matrix air permeabilities ($m^2 \times 10^{-16}$).

	Suction (kPa)						
	10	25	50	100	300	500	Oven Dried
Mean	1.54	11.20	16.88	26.67	35.11	38.23	57.12
C.V., %	434	436	344	326	309	295	272
Minimum	<0.01	<0.01	0.02	0.25	1.29	1.91	3.81
Median	0.05	0.10	0.39	2.10	5.09	6.04	12.08
Maximum	41.90	333.10	389.80	678.70	780.50	780.50	1012.60

Data from laboratory saturated hydraulic conductivity and laboratory oven-dried pneumatic permeability are used to calculate the Klinkenberg coefficient and equivalent pore sizes of oven-dried cores for nitrogen gas at mean air pressures of 108 kPa and an assumed mean free path of 9×10^{-8} m. Table 13 presents summaries of the observed values. The data varies from a low of 35 kPa to a high of 1277 kPa, with a mean of approximately 322 kPa.

Table 13: Summary of laboratory determined Klinkenberg slip flow coefficient.

	KLINKENBERG COEFFICIENT (kPa)
Mean	322.
C.V., %	82.
Minimum	35.
Median	217.
Maximum	1277.

Field Pneumatic Properties

Field estimates of pneumatic permeabilities are obtained using single hole air injection tests over three meter intervals corresponding to sample locations coincident with laboratory core segment tests and field hydraulic tests. The field test procedure consists of locating two inflatable packers at either end of a test interval, inflating the packers to isolate the test interval, injecting a controlled mass flow rate of air into the interval, and measuring the absolute pressure in the injection interval. The air permeability is calculated using the Dachler equation adapted for compressible air flow. The analytic solution assumes that the test medium is homogeneous in the vicinity of the test interval, and that no leakage around the packers occurs. Also, the assumption is made that no air leakage through the rock into the borehole above or below the packers is occurring. Flow rate is in standard cubic meters per second, which has been adjusted from a mass flow rate using standard temperature and pressure.

Table 14 summarizes results of the single hole pneumatic tests. As noted earlier, calculated laboratory air permeabilities are greater than laboratory water permeabilities which is consistent with the Klinkenberg effect. Unlike the laboratory results, however, field estimated air permeability is lower than the field estimated water permeability. This difference can most likely be attributed to the presence of water in the rock, which is not the case for an oven-dried sample.

Table 14: Summary of field determined air permeability.

	FIELD PNEUMATIC PERMEABILITY ($m^2 \times 10^{-16}$)
Mean	178.1
C.V., %	667
Minimum	< 0.42
Median	4.02
Maximum	> 13,366.

NOTE: One interval exceeded capacity of measurement device, while a second interval was less than the measurement threshold.

3.4 Thermal Characterization Parameters

Thermal gradients can substantially affect the movement of water as liquid and vapor in the subsurface. Characterization of thermal sources and sinks as well as the moisture dependent thermal properties of the rock matrix and fractures is important for modeling thermal effects on fluid and solute transport. This section presents laboratory and field data sets for thermal parameters corresponding to sample locations consistent with other data sets presented in this report.

Matrix Thermal Properties

Thermal properties of the rock matrix are estimated by drilling two holes in the large core segments. The holes are 0.36 cm in diameter, one hole lying along the radial axis of the core segment extending into the rock 4.5 cm. The second hole lies approximately 0.7 cm from the central hole and extends 2.5 cm into the core. After the core has equilibrated at a constant matric suction, liquid mercury at room temperature is added to each hole until the level of mercury is slightly below the core surface. A heating unit composed of precision resistance wire wrapped around a copper wire core is placed in the central hole. A thermistor probe is placed near the bottom of the outer hole. The rock is then placed within an insulating plexiglas chamber which fits snugly around the core. The entire apparatus is then placed within a constant temperature chamber. A known electric current is used to heat the unit in the central hole for approximately 150 seconds. A response to the heating event is observed in the outer hole, the magnitude of which is used to evaluate the thermal diffusivity, conductivity and heat capacity of the sample for each water content. The parameters are determined using a radial flow equation. Table 15 summarizes laboratory thermal properties.

Table 15: Summary of laboratory thermal conductivity (W m^{-1} K^{-1}).

	Suction (kPa)							Oven
	0	10	25	50	100	300	500	Dried
Mean	1.821	1.800	1.820	1.775	1.817	1.729	1.727	1.266
C.V., %	10.7	9.2	10.6	11.8	11.8	11.4	10.7	11.5
Minimum	1.291	1.381	1.464	1.356	1.382	1.445	1.095	0.829
Median	1.839	1.792	1.801	1.758	1.779	1.696	1.717	1.281
Maximum	2.491	2.484	2.580	3.568	2.785	2.575	2.138	1.966

Field Thermal Properties

Potential sources of thermal effects in the unsaturated zone near a HLW repository include heating at the ground surface, the geothermal gradient from below, repository waste decay, and latent heating due to phase changes. Surface heating effects result from annual and daily solar cycles, while the geothermal gradient results from heat flux from depth. For the ALTS data set, the effects of daily solar cycles and latent heating are not easily detected and waste decay is not relevant. Only the effects of an annual solar cycle and the geothermal gradient are readily apparent. The geothermal gradient, in turn, appears to be constant, approximating 0.03 K m^{-1}. Without a measure of the heat flux, however, no estimate of thermal properties can be determined.

The effects of an annual solar cycle can be used to estimate thermal diffusivity at ambient conditions. Carslaw and Jaeger (1959) present an analytic solution for the temperature distribution in a semi-infinite solid in response to a steady harmonic heating source. For the ALTS, one estimate of the thermal diffusivity can be obtained using the phase shift with depth. Borehole temperatures were measured using thermistors placed at one meter intervals and allowed to equilibrate with the host rock. By assuming a solar maximum near July 10, and by noting the depth at which the temperature is a maximum for a given date, effective thermal diffusivities of 0.81, 0.23, 0.57, and 0.35 x 10^{-6} m^2 s^{-1} are estimated using data for 4/22/87, 12/18/87, 3/23/88 and 12/10/88.

The field thermal diffusivity value can be compared with data for laboratory cores. Assuming a thermal conductivity of 1.95 W m^{-1} K^{-1} and a saturated heat capacity of 2.4 x 10^6 J m^{-3} K^{-1}, a thermal diffusivity of 0.81 x 10^{-6} m^2 s^{-1} is estimated, which compares favorably with the field results, above. The mathematical model will not exactly replicate the physical system, however. In particular, the driving force is not an exact harmonic and the date of the assumed maximum is not accurate. Also, the thermal diffusivity is not a constant, but varies spatially and temporally due to changes in material properties and moisture content.

3.5 Quantification of Parameter Uncertainties

Due to large spatial and temporal variations in parameters which describe the hydrogeology and geochemistry of subsurface media, the determination of factors which result in uncertain parameter estimates is an important component of site characterization. The variability may be induced naturally or may be due to measurement errors, either case resulting in parameter uncertainty. Identification of the source of the uncertainty is particularly important for providing mitigating measures, and for correctly characterizing the variability.

Uncertainties result from natural geologic variability, from improper measurements, from inaccurate instruments or from factors that are not controlled. The effect of the uncertainty is to reduce the confidence in a proposed conceptual model or to result in the incorrect specification of a conceptual model. Sources of uncertainty have been characterized with regard to the degree of uncertainty introduced in data collection and interpretation as well as the influence of the uncertainty on system performance.

Because uncertainties may arise due to natural variability in the subsurface, the influence of natural variability can be difficult to distinguish from instrument error. Changing the scale over which a parameter is measured often can change the interpreted value of a parameter, especially for heterogeneous materials. Averaging over larger volumes may result in more stable parameter estimates but at the cost of predictive capability over smaller regions.

System performance may not be correctly determined if system parameters are not measured with sufficient precision. For example, the determination of a hydraulic conductivity curve which relates the hydraulic conductivity of a sample to the fluid content is critically dependent on precise measurements. If such measurements are not performed with sufficient precision the application of the derived curve will not provide accurate flow rates. Equally important is the accuracy of the technique employed. Errors resulting from neglecting controlling factors, such as temperature, power supply voltage for control or monitoring equipment, human, or methodological errors can bias parameter estimates so that predictions and interpretations are incorrect.

Relative Magnitude and Propagation of Errors

Identification and order-of-magnitude quantification of various components of uncertainties has been performed using procedures to replicate, duplicate, and provide redundant measurements for each parameter. Replication involves the repeated sampling using a single instrument on the same sample. The purpose of replicated sampling is to provide estimates of the precision of the measurement technique, as well as to characterize spatial variability. Influences such as temperature can be monitored and an analysis can be performed to determine their effects. Duplication is the use of a number of identical instruments to measure a specific sample. Variability induced by inaccurate instruments can be determined using this

technique. Redundancy involves the use of various methods to determine the same parameter. By estimating parameters using independent techniques, estimates of methodological bias can be obtained. In addition, systematic errors induced by ignoring controlling variables can be examined. This is possible because each technique may not respond in the same manner to the controlling variable.

Estimation of Parameter Uncertainties

To demonstrate representative parameter uncertainty analyses, four parameters were evaluated using repetition and duplication procedures. Rasmussen et al. (1990) present data for interstitial, hydraulic, pneumatic, and thermal properties for 105 core samples taken at regular intervals from boreholes at the Apache Leap Tuff Site.

Dry air permeability was estimated for three control samples in two different permeameters on various dates. Large core samples GA, JA, and MA were repeated in different permeameters, with the coefficient of variation for Permeameters 1 and 2 being computed for Sample GA. The air permeability values measured at two separate times are compared for Sample EH. The results of these experiments are presented as Table 16. Saturated hydraulic conductivity tests on large core samples AC and AE were repeated in different permeameters. Sample EA has an additional determination 5 months later. Results for the saturated hydraulic conductivity tests are presented as Table 17.

Table 18 presents relative saturation data reported in Rasmussen et al. (1990) for two samples. The coefficient of variation for the effective porosity is approximately three to four percent. The reported coefficient of variation in effective porosity reported for all samples was approximately thirteen percent. If the assumption can be made that the measurement error is independent of geologic variations then the total variance is the sum of the geologic variation plus the measurement variance, i.e.,

$$\sigma_T^2 = \sigma_G^2 + \sigma_M^2$$

where σ_T^2 is the total observed variance, σ_M^2 is the measurement variance, and σ_G^2 is the geologic variance. Using the independence assumption, it can be concluded that the geologic coefficient of variation for effective porosity is about eight times the measurement error.

Unsaturated hydraulic conductivity tests for one of two samples, GC or UC, were run once every tenth sample. Sample GC was tested in one permeameter, while sample UC was rotated between four different permeameters. The test data, presented in Table 19, indicate that the coefficient of variation remained fairly constant, between 32 and 48 percent, for the sample tested in the same permeameter, while the sample tested in different permeameters showed a greater variation, between 9 and 78 percent.

Table 16: Oven dry air permeability for parameter variation estimation.

Sample	Permeameter	Date	Air Permeability ($m^2 \times 10^{-16}$)	Mean ($m^2 \times 10^{-16}$)	Coef. Var. (%)
GA	1	11/3/87	7.40		
	1	11/5/87	6.89		
	1	11/5/87	6.82	7.04	4.50
	2	11/4/87	5.48		
	2	11/5/87	5.23		
	2	11/6/87	5.09	5.27	3.75
			For all permeameters:	6.15	16.22
JA	1	11/5/87	6.28		
	2	11/5/87	5.36		
	3	11/5/87	5.66		
	3	11/5/87	5.69		
	1	11/6/87	6.44		
			For all permeameters:	5.89	7.72
MA	1	11/3/87	7.55		
	2	11/3/87	6.86		
	2	11/3/87	6.79		
	3	11/5/87	6.83		
	1	11/6/87	7.77		
			For all permeameters:	7.16	6.48
EH	3	1/31/88	9.49		
	2	1/31/88	9.53		
	2	4/25/88	9.37		
			For all permeameters:	9.46	0.88

Table 17: Saturated hydraulic permeability for parameter variation estimation.

Sample	Permeameter	Date	Hydraulic Permeability ($m^2 \times 10^{-16}$)	Mean ($m^2 \times 10^{-16}$)	Coef.Var. (%)
AC	1	11/16/87	2.10		
	2	11/16/87	2.05		
	3	11/16/87	1.91		
	3	11/19/87	2.09		
			For all permeameters:	2.04	4.30
AE	2	11/16/87	0.88		
	3	11/17/87	0.84		
	1	11/18/87	1.02		
	1	11/18/87	0.93		
	3	11/19/87	1.02		
			For all permeameters:	0.94	8.67
EA	3	11/16/87	6.62		
	1	11/18/87	6.57		
	2	11/19/87	6.57		
	2	11/19/87	5.92		
	3	4/28/88	5.36		
			For all permeameters:	6.04	10.59

Table 18: Moisture characteristic curves for parameter variation estimation.

Sample	Effective Porosity	RELATIVE SATURATION (%) Suction (kPa) 10	25	50	100	300	500
SA	0.150	99.37	98.51	95.17	68.94	60.77	53.63
	0.165	99.55	98.49	96.28	70.44	51.61*	43.73*
	0.157	99.87	99.78	95.95	68.02	49.72*	43.75*
Mean	0.158	99.60	98.63	95.80	69.13	54.04	47.04
C.V., %	3.9	0.2	0.6	0.5	1.4	8.9	9.9

Sample	Effective Porosity	RELATIVE SATURATION (%) Suction (kPa) 10	25	50	100	300	500
UA	0.160	99.74	97.78	96.25	78.43	73.53	67.14
	0.172	99.60	98.97	97.47	78.10	57.75*	47.27*
	0.164	100.00	98.85	97.25	77.62	54.83*	48.38*
Mean	0.165	99.87	98.85	96.99	78.05	62.03	54.26
C.V., %	3.2	0.3	0.8	0.6	0.4	13.2	16.8

* Different pressure plate used.

Table 19: Unsaturated hydraulic conductivity values for parameter variation estimation. Sample GC tested in same permeameter. Sample UC tested in four different permeameters.

	UNSATURATED HYDRAULIC CONDUCTIVITY ($m\ s^{-1} \times 10^{-6}$)			
	Suction (kPa)			
Sample	10	25	50	100
GC	1.127	0.759	1.106	0.569
	2.407	1.711	0.974	0.886
	2.745	2.744	1.928	0.813
	1.658	1.596	0.731	0.424
Mean	1.984	1.703	1.185	0.673
C.V., %	37	48	44	32

	UNSATURATED HYDRAULIC CONDUCTIVITY ($m\ s^{-1} \times 10^{-6}$)			
	Suction (kPa)			
Sample	10	25	50	100
UC	2.623	3.040	2.507	1.014
	6.214	4.649	2.616	0.883
	9.523	5.972	2.070	0.978
	1.512	15.700	1.705	1.105
Mean	4.968	7.340	2.225	0.995
C.V., %	73	78	19	9

4. UNSATURATED ZONE SAMPLING AND MONITORING

4.1 Liquid and Vapor Water Sampling

The movement of water through unsaturated geologic media is made possible both by migration within an interconnected liquid phase as well as through air-filled voids in the vapor phase. Vapor transport may be especially important in regions where the liquid phase transport is small and the proportion of air-filled voids is large. Vapor phase flow may also be important across open fractures due to small separation distances. Vapor flow across open fractures is important in that dissolved solutes will be left behind on the influent fracture surface. While this process will result in solute retardation, subsequent saturation of the fracture may remobilize the concentrated solutes and result in enhanced solute transport. The proper identification of vapor and liquid flow characteristics is therefore critical for understanding solute transport processes in unsaturated fractured rock. Green and Evans (1987) discuss the relevance of various vapor transport processes in unsaturated fractured media.

It is commonly recognized that the presence of fractures substantially complicates models of fluid and solute transport in unsaturated geologic materials. While the significance of liquid flow through unsaturated fractures has been widely acknowledged, the relative importance of vapor flow has been commonly overlooked. Substantial research into coupled liquid-vapor flow, especially under non-isothermal conditions, has not been performed and has only recently been examined.

Smith (1989) measured significant natural airflow in two boreholes tapping unsaturated fractured tuff at the ALTS. To provide reference data sets and analyses of vapor flow through discrete fractures, a borehole at the Apache Leap Tuff Site was instrumented with an air velocity meter in conjunction with a relative humidity sensor and a temperature probe (Figure 7). The borehole selected displayed the greatest air movement of the existing boreholes, the air movement being directly related to the presence of a single large fracture. Flow rate and direction through the more productive hole and atmospheric pressure and temperature were monitored during periods from December 1987 through June 1988 (Figure 8). A strong correlation between flow velocity and atmospheric pressure exists at time scales of minutes to months, while the effect of temperature on flow is manifested by a seasonal reversal in net flow direction. Net outward flow occurs in winter, reversing to net inward flow by late spring. The observed flow pattern is consistent with that observed at Yucca Mountain, Nevada, which is similar both lithologically and topographically to the ALTS.

Outflow of fracture air was associated with high relative humidities, and associated high rates of vapor movement from the fracture to the atmosphere. Inflow of air to the fracture was associated with low humidities, and the inferred evaporation of water from fracture surfaces. Regional estimates of vapor loss to the atmosphere through fractures were not possible due to the selective nature of the measurements.

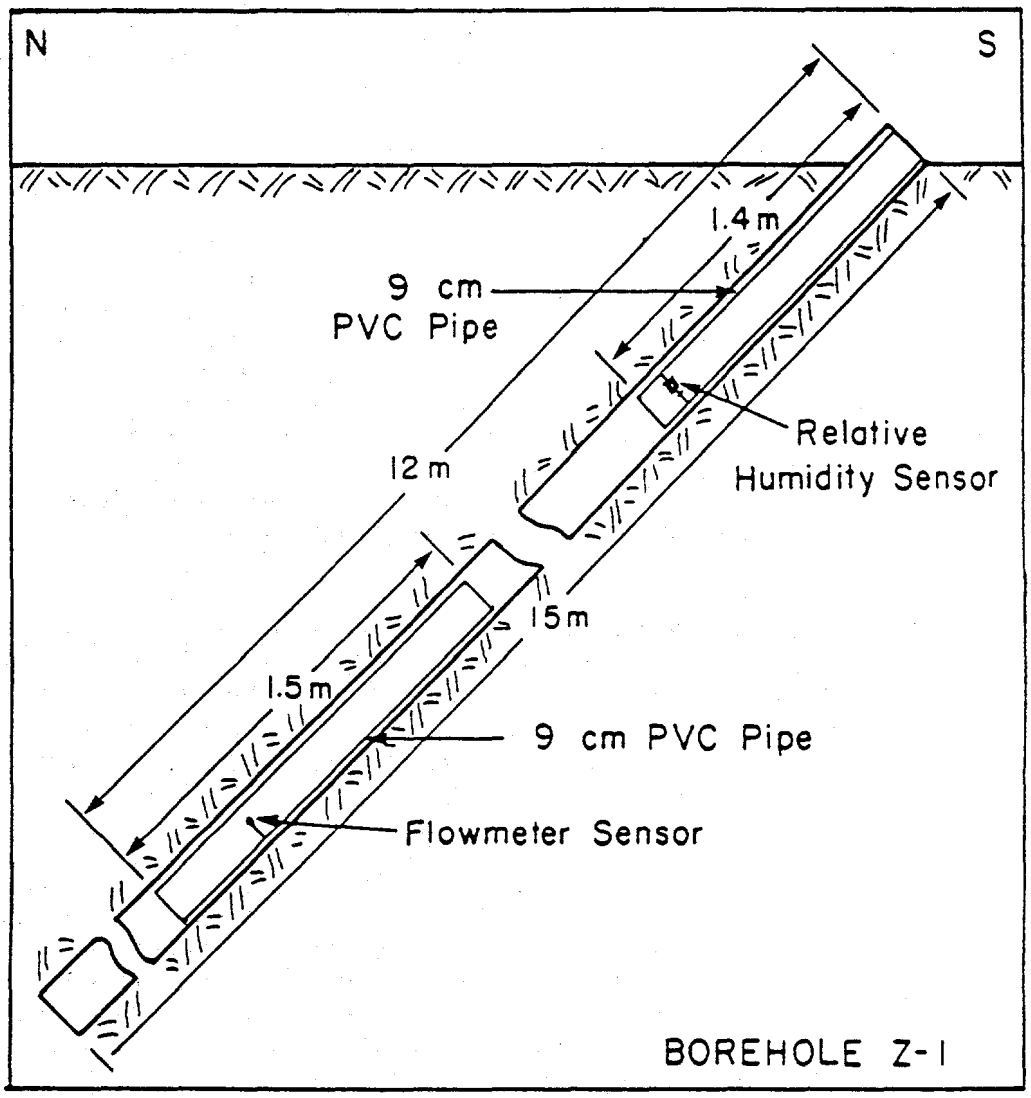

Figure 7: Experimental setup used to measure airflow and temperature in Borehole Z-1 at ALTS.

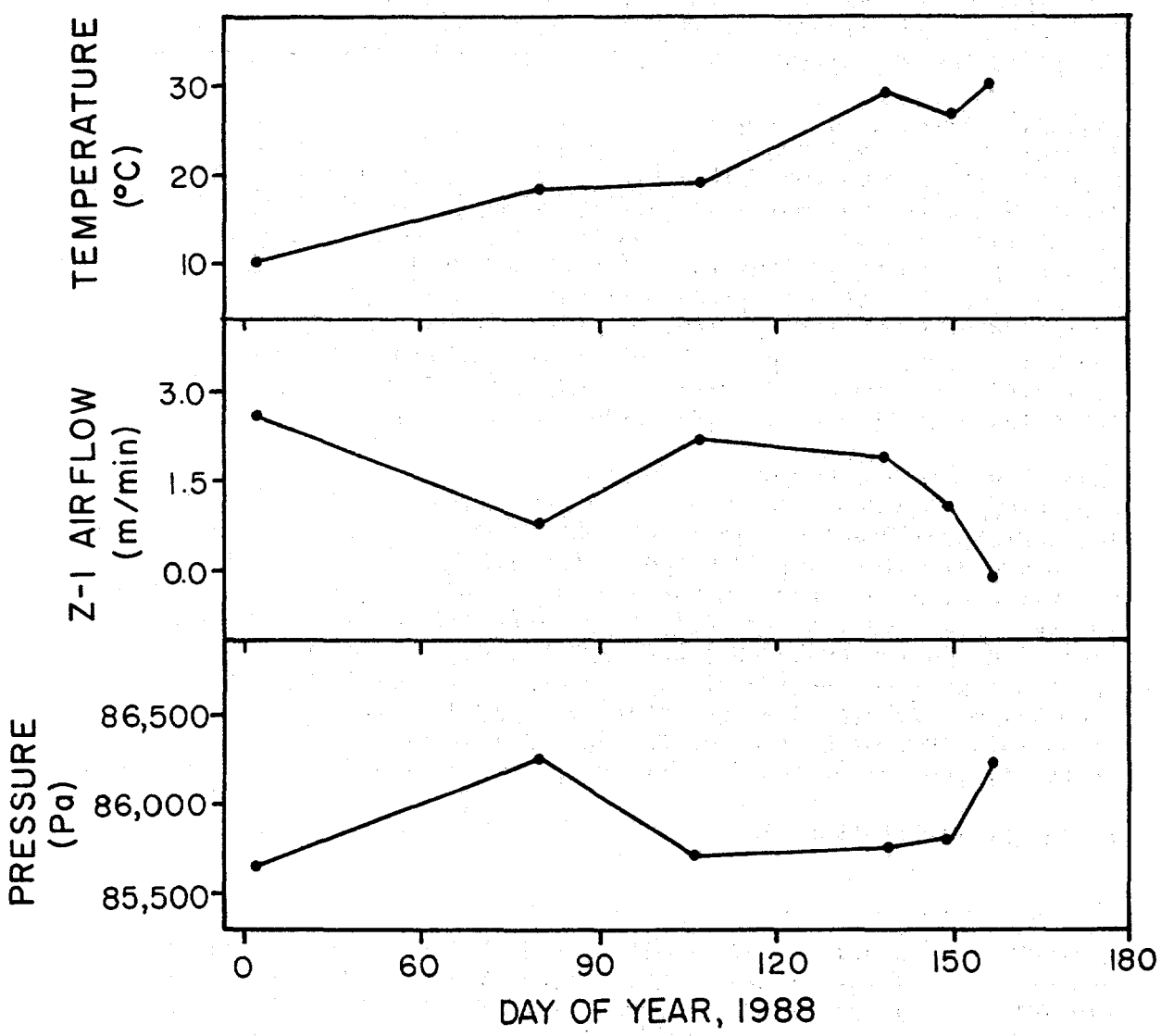

Figure 8: Average values of temperature, airflow velocity, and atmospheric pressure versus date.

Direct sampling techniques have been developed for collecting in situ samples of both liquid and vapor. Laboratory sampling methods have been developed for measuring the concentration of tracers used in studies of fluid movement through fractures and the rock matrix in tuff block samples. Adequate volumes of water are obtained for ion specific electrode analysis by inserting absorbent membranes into sampling ports which have sufficient capillary suction to wet the membrane. When removed from the sampling ports, the membranes provide a saturated medium for electropotential measurements. The membrane is removed from the sampling port and is quickly placed in position for analysis. A previously calibrated coated wire electrode is placed in contact with the membrane surface to determine the electrochemical potential. A measurement can then be made of the concentration of the specific ion that was used as the tracer. A wide variety of electrodes are available for specific ions of interest (Figure 9).

The laboratory method works satisfactorily if the water is in a liquid form (even as a thin film). Efforts must be made, however, to prevent rapid evaporation of the membrane which if not controlled will cause errors due to changing solute concentration. Details of the method are reported by Chuang et al. (1990). The precision obtained using the coated wire electrode is affected by the saturation of the sampling membrane and by leakage of filling solution from the reference electrode. While it was not possible to measure concentrations more precisely than twenty percent, tracer breakthrough curves were clearly detectable by measuring sequential samples.

Field sampling techniques have been limited to collection of spring discharge from tuff sections which provide samples that represent primarily fracture discharge. Samples collected from springs are of sufficient volume to allow a complete standard chemical analysis using established methods. Most of the fluid moving through the full section at the Apache Leap Site occurs as unsaturated flow. The observed springs and seeps represent the discharge from large sections of the tuff. To date, no fluid experiments have been conducted which would require in situ unsaturated zone sampling.

Vapor phase sampling using the ion specific electrode has not been attempted, primarily because most tracers used have insufficient vapor pressure. Condensation of vapor samples is possible, however, with analyses restricted to constituents with high vapor pressures such as many organic compounds and the various isotopes, natural and artificial, present in water. These tests would not be possible using the ion-specific electrode, however, and would require more expensive laboratory procedures.

4.2 Ground-Water Recharge, Infiltration and Deep Percolation

Recharge of downward percolating water in the unsaturated zone across the water table may or may not be uniformly distributed in space or in time. Infiltration at the earth's surface is distributed unevenly in both space and time, but the variations may be attenuated rapidly with depth. Variations in discharges from seepage faces in the unsaturated zone can

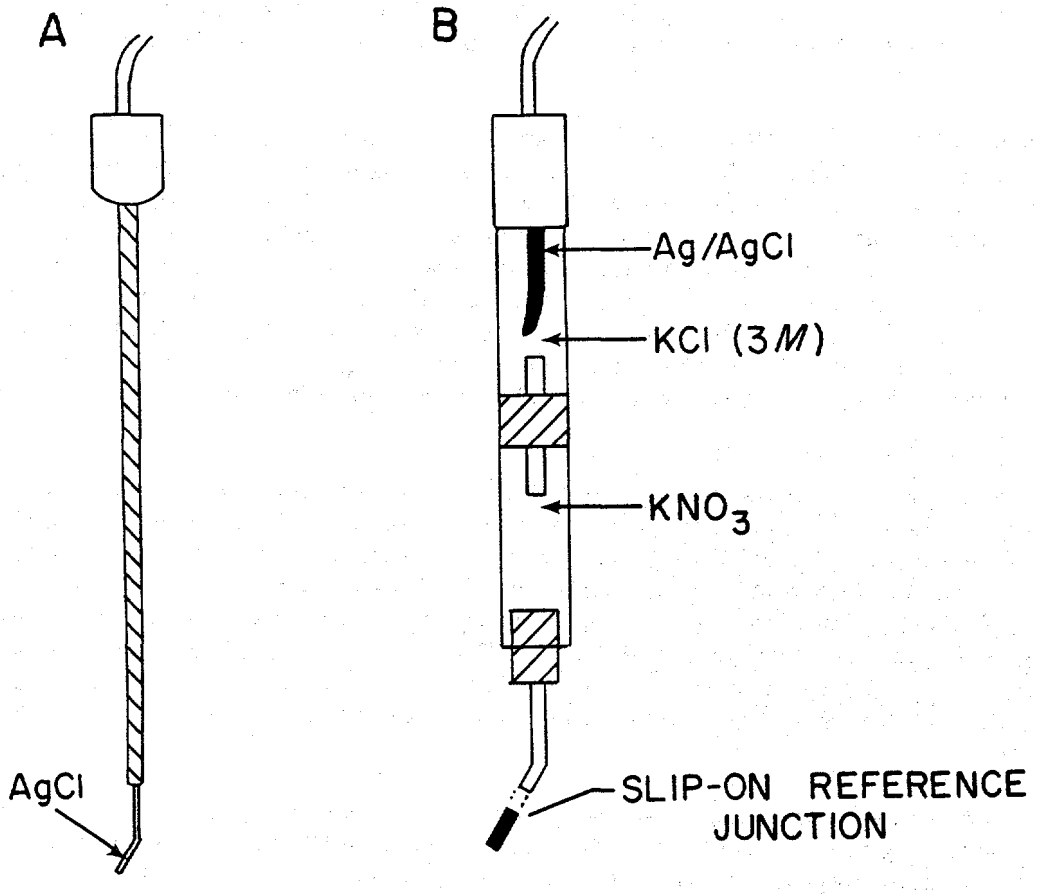

Figure 9: Specific ion electrodes used to measure solute concentration in water absorbed from the rock matrix and fracture using filter paper.

display substantial variability, even at great depth, however. The downward percolation of water within the rock matrix may remain more constant than flow through embedded fractures. Rasmussen and Evans (1989) demonstrate that zones of positive pressure will exist in vertical fractures even when matric suctions are generally present. Simulated travel times and fluid velocities through vertical fractures may be unaffected as the fracture saturation decreases, depending upon the functional form of unsaturated fracture hydraulic properties. These results support field observations of flowing fractures in unsaturated rock. Of specific interest are the conditions that promote and inhibit fracture flows under conditions where the matric suction in the rock matrix would indicate that all fractures should be drained.

Computer models employed to characterize flow through the unsaturated zone generally require the specification of boundary conditions. As a rule, the fluid flux at the upper boundary (i.e., at the ground surface) is defined using field observations of flow rates below the root zone, or using the difference between regional precipitation estimates and regional actual evapotranspiration estimates. Both techniques are compromised by measurement errors as well as variations in space and time. To assess the sensitivity of boundary fluxes to estimation techniques, field data at the Apache Leap Tuff Site have been used to estimate errors and biases (Rasmussen et al., 1990). The study presents neutron count data in conjunction with laboratory relative permeability data to evaluate the magnitude of matrix percolation rates. Additional data are available from watershed studies designed to estimate the magnitude of various surface infiltration phenomena including precipitation and runoff variation.

The movement of water through the unsaturated zone begins with the infiltration of water at the ground surface. Prior to this action, water will have fallen (measured as precipitation), been intercepted by vegetation, been subject to surface storage, and flowed across the ground surface (measured as runoff). Infiltration can be estimated by subtracting runoff from precipitation. This estimate represents an average over the catchment area, and may be biased due to the failure to include interception and evaporation losses. Increased infiltration may be present in regions where water accumulates, as well as in materials with enhanced infiltration characteristics. The infiltration will not be constant over time, and will vary with season, rainfall intensity and duration, form of precipitation (snow vs. rain), and time of day.

Once the water has moved into the subsurface, water uptake by roots to meet plant transpiration needs, and vapor pressure gradients, will result in the return of water to the atmosphere. This process, termed actual evapotranspiration, will reduce the amount of percolating water; the residual downward-moving water below the root zone being called deep percolation. Ground water recharge occurs once the deep percolation component reaches the water table. Processes which may prevent the deep percolation component from recharging ground water include vapor flow to the atmosphere and horizontal flows to the ground surface where the water is discharged as springs.

Ground water recharge estimates based on a water budget approach which attempts to calculate the various components and losses are subject to cumulative errors which may be many times greater than the amount of recharge being estimated. Uncertainties with respect to the spatial and temporal variabilities render most such estimates useless, especially when the recharge amount is small.

Estimates of ground water recharge can also be based on neutron count data, water content vs. neutron count calibration curves, and water content vs. unsaturated hydraulic conductivity relationships. The procedure consists of measuring neutron counts in the field below the root zone. A procedure is then developed for calibrating neutron counts with in situ water content. Rock samples are then tested in a laboratory to determine the unsaturated hydraulic conductivity at the observed field water content. If a unit hydraulic gradient is assumed, then the unsaturated hydraulic conductivity should equal the deep percolation rate.

Elder (1988) provides calibration data sets which relate neutron moisture probe counts to volumetric water content. Neutron probe calibration is a function of the design of the probe, the geometry of the access hole, and the composition of the material. It is typically derived from an empirical relationship between counts of neutrons and known water contents. For consolidated rocks, this empirical calibration is difficult. A calibration procedure based on a numerical model of a neutron probe is developed to overcome the difficulties. The theory behind the model is the Three Group Diffusion theory. The input parameters are the probes's design, the material properties plus neutron cross sections, and the geometric proportionality factors for the access hole. The neutron cross sections are determined using a graphite pile. The calibration is sensitive to the material's bulk density, thermal absorption and scattering cross sections. With this procedure a neutron probe may be calibrated to any geologic material.

Errors in this approach include the difficulties associated with developing a calibration between neutron counts and the field water content, as well as in estimating a representative unsaturated hydraulic conductivity at the water content of interest. The calibration curve is made difficult by the inability to extract a rock sample without substantially altering its initial water content. The unsaturated hydraulic conductivity estimate will be uncertain because fractures will have been excluded by most tests and the resulting estimate may substantially underestimate the true value. Episodic infiltration events may not be sampled because of the infrequency in space and time of flows through individual fractures.

Brown (1986) examined the potential for estimating steady recharge to deep unconfined aquifers by comparing observed water levels to the water levels produced by a series of simulated cases. An analytical solution to the Boussinesq equation was found to give a poor estimate of water table position and hence recharge. To obtain better estimates of recharge rates based on water table configurations, finite-element simulations were performed on an idealized region to examine the sensitivity of the water table position to anisotropy, recharge, grid density, horizontal layering,

and region geometry. The position of the water table was found to be particularly sensitive to region geometry, medium heterogeneity and anisotropy. A graphical method based on comparison of water levels at three observation points to simulated water levels produced a good estimate of dimensionless recharge and the anisotropy ratio. Determination of the absolute value of recharge requires accurate determination of region geometry and hydraulic conductivity so that computer simulations are representative.

5. CHARACTERIZATION USING GROUND-WATER CHEMISTRY

Hydraulic tests of fractured materials result in estimates of parameters relevant to the prediction of flow paths and travel times. Confirmation of the predictions is required in order to validate the test procedures and the models used in the prediction process. Geochemical information provides an important additional source of data for evaluating the adequacy of the prediction models. Information such as residence times and rates of solute movement may be obtained using geochemical information. At the Apache Leap Site the ground water is below the tuff in a carbonate section and no wells are open for sampling. Numerous drill holes are located in the area but access is limited in some areas due to private ownership of the holes. The presence of a mine haulage tunnel within the Apache Leap Tuff near the field site has afforded the opportunity of collecting water flowing through open fractures.

Samples of minerals for stable isotope analysis have provided data clearly indicating that meteoric water at ambient temperature has caused much of the alteration within the tuff, but the rate and timing will not be known without more detailed studies, such as radiometric dating. The work of Weber and Evans (1988) and Rogoff (1988) provide valuable data regarding the formation of secondary minerals. Their work examines the isotopic shift of the altered rock as compared to whole rock and unaltered rock sections. Rogoff shows that phenocrysts of biotite and hornblende located near a fracture had been altered by cool meteoric water rather than by hot fluids associated with the formation of the tuff flows. Not yet known, however, is how rapidly the water moves through the tuff section.

Weber and Evans (1988) identify stable isotope variation and mineralogical changes in fractured rock to establish the history of climatic and geomorphological processes that might affect the isolation properties of a waste repository. This study examines the use of the stable isotope ratios of oxygen ($^{18}O/^{16}O$) and carbon ($^{13}C/^{12}C$) in authigenic minerals as hydrogeochemical tools tracing low-temperature rock-water interaction in variably saturated fractured tuff. Isotopic compositions of fracture-filling and rock matrix minerals in the Apache Leap tuff are concordant with geothermal temperatures and in equilibrium with water isotopically similar to present day meteoric water and ground water. Oxygen and carbon isotope ratios of fracture-fillings, in unsaturated fractured tuff, display an isotopic gradient probably resulting from near-surface isotopic enrichment due to evaporation rather than the effects of rock-water interaction. Oxygen isotope ratios of rock matrix opal samples exhibit an isotopic gradient due to leaching and reprecipitation of silica at depth. Results can be used to further define primary flowpaths and the movement of water in variably saturated fractured rock.

Rogoff (1988) reports alteration of rock by water in all levels of the Apache Leap Tuff. Possible alteration conditions range from hydrothermal circulation after eruption of the tuff to percolation of low temperature modern water. This study uses stable isotopes of oxygen and hydrogen in matrix phenocrysts and whole rocks to determine temperature and timing of alteration, and the extent of water-rock interaction at progressive

distance from fractures. The data indicate low temperatures (20 to 30 °C) of water-rock interaction. Water-rock ratios increase stratigraphically upward. Water-rock ratios also decrease as distance from fractures decrease, suggesting that fractures may not have been major flow conduits. Calculations indicate a water oxygen isotopic composition similar to modern water, although the water hydrogen isotopic composition is heavier than modern water due to evaporation.

Geochemical sampling has been performed in the field by collecting rock, minerals and fracture wall coatings for isotopic analysis. Samples have been analyzed for stable isotopic ratios ($^{18}O/^{16}O$, D/H, $^{13}C/^{12}C$) and for mineralogy. Weathering profiles are indicated by an isotopic shift. Values for $\delta^{18}O$ and δD clearly demonstrate that low temperature fluid has moved through the tuff matrix and altered the glass minerals to clays. Additionally, secondary minerals present in the fractures represent precipitation from recharging fluids. It is clear that samples of rock and mineral material can be collected to obtain stable isotope analyses as well as to show that the observed fractionation is large enough to indicate weathering and secondary precipitation.

Rock samples have also been collected from core materials and from drill holes at predetermined distances from natural fractures. Preliminary evidence indicates that whole rock and phenocrysts are being altered by fluid passing through the rock. Of concern is whether fluid moves from the fracture into the matrix and therefore leaves an alteration profile of decreased weathering and reaction toward the matrix, or whether fluid moves from the matrix into the fracture. While too few samples have been collected to determine the direction of flow for the reacting fluids, additional sample collection can be used to resolve this issue.

5.1 Chemical Evolution of Waters in the Apache Leap Tuff

This section contains a discussion of preliminary results from research involving examination of the chemistry of aqueous systems in an unsaturated fractured rock. Objectives include characterization of the chemical environment and identification of processes altering the chemistry of waters that begin as precipitation then flow through fractures in the Apache Leap Tuff. Some possible flow paths are hypothesized, based upon local geology and relative geographic positions of surface water. With chemical analyses of rain waters and of waters at the beginnings and ends of these hypothesized flow paths, they will be verified or replaced with alternatives.

With unsaturated thicknesses of 100 m to over 1000 m, ALTS overlies an extensive volume of rock containing unsaturated fracture flow systems. As expected, springs in the region are rare except in shallow alluvial flow systems, such as the Queen Creek bed, and in recent years have become even more scarce. Two springs in the Apache Leap Tuff, 2.3 and 3.5 km northeast of town of Superior, ceased flowing in 1972.

One spring in the lower part of the White Unit of the tuff has continued to flow intermittently. Located 0.5 km east of Highway 60, water flows from a

fracture in the tuff into a spring box built into a cliff about 10 m above the canyon floor. Although the source of this water is uncertain, relative geographic proximity suggests that it may be a pond located 500 m southwest and 25 m above the spring. If indeed this hypothesis can be verified, and the two surface water bodies are connected by a water bearing fracture, accessibility of water samples from the origin and endpoint of the fracture flow path will render the system useful for chemical evolution analyses.

ALTS overlies Magma Mine, a network of tunnels and shafts that provides unusual access to subsurface waters in fracture flow systems. One mine tunnel has provided underground access to the lower units of the tuff formation. The tunnel at the 500 level (500 ft below a reference elevation of 3569 ft) traces a curved path from the town of Superior to a point within 500 m of ALTS, a total distance of 2830 m (Figure 10). Although the western portion is in limestone units underlying Apache Leap Tuff, over half of the tunnel passes through tuff. The tunnel roughly parallels Queen Creek, the major drainage of the region, and passes directly under it at a point 700 m from its eastern end, where creek and tunnel diverge. Proximity to Queen Creek may be critical to availability of source water for flow into the tunnel. Tunnel depths below surface vary from 0 m at the tunnel's western end to 370 m near the east end termination. At their closest point, the tunnel lies 110 m directly below the creek.

Potential corridors for flow connect Queen Creek with the tunnel. As is typical of the tuff, rock in the tunnel/creek region is cut by parallel fracture systems, most of which trend roughly N-S. A fault zone traces a N-S path that crosses Queen Creek and may intersect the tunnel below. The expanse of fractured rock between Queen Creek and the 500-level mine tunnel is a second hypothesized flow system for which initial water chemistry and final water chemistry may be determined and used for chemical evolution analysis.

5.2 Estimation of Fracture Water Travel Times

Contact time with the mineral phases in an aqueous system is one factor that influences a water's chemistry. Those waters with relatively long contact times are more likely to have reached chemical equilibrium with surrounding minerals than those that have reacted with a given mineral assemblage for a shorter period of time. Measurements of fracture water travel time can be made knowing the time between availability of source water at the surface above the fracture and arrival of that water at a point along the fracture. Optimally this estimate is made for an initially dry fracture knowing the time of first arrival of water at a given point and the starting time of an isolated surface runoff event.

For the hypothesized Queen Creek-mine tunnel fracture flow system, Queen Creek is the source of surface water and the mine tunnel is the system end point. Logistically, precise measurements as described above are unfeasible here, but with historical data the approach is useful for obtaining more general travel time estimates. Figure 11 presents graphs that represent relative monthly volumes of water present as precipitation, Queen Creek discharge, and influx to Magma Mine during a 72 month period.

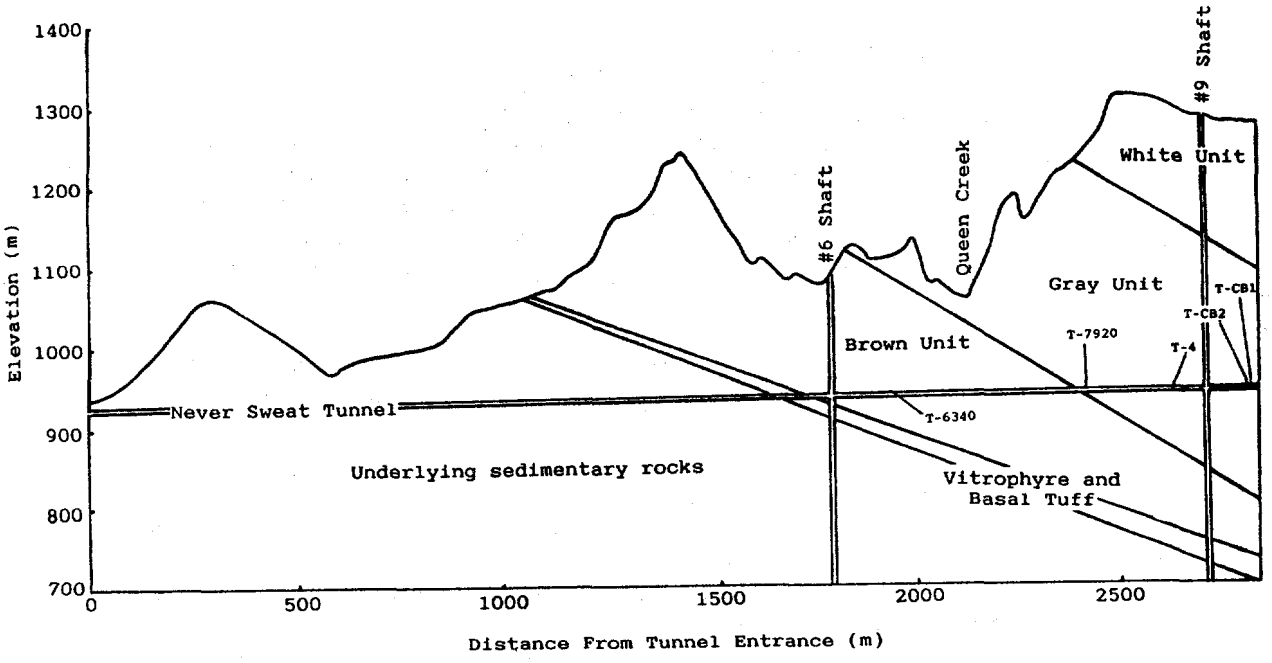

Figure 10: Linear profile of Magma Mine's Never Sweat Tunnel showing overlying topography, geology, intersecting mine shafts, and location of sampling points.

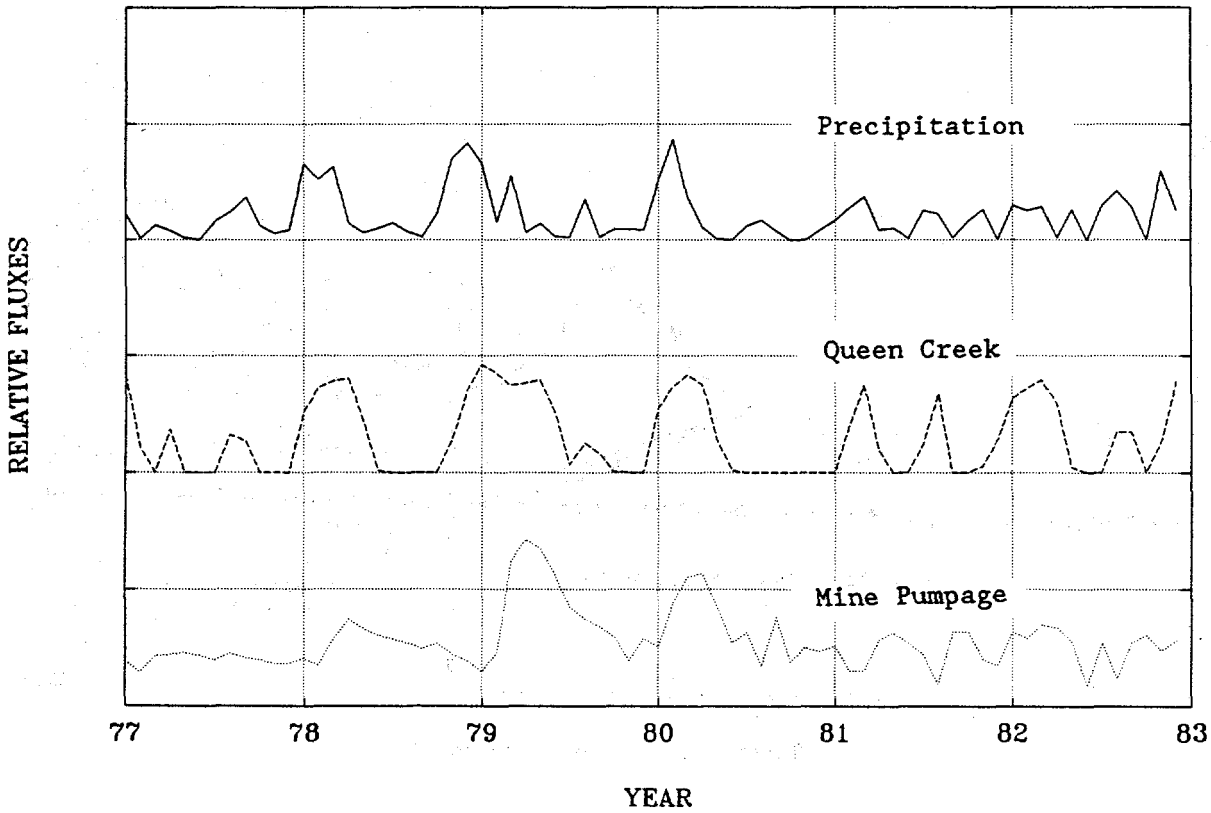

Figure 11: Graphs of atmospheric precipitation at Superior, water diversions from Queen Creek, and Magma Mine pumpage volumes.

Increased mine pumping is clearly associated with periods of high stream discharge and rainfall. Because temporal displacements between Queen Creek pumping peaks and mine pumping peaks vary from 0 to 3 months, average travel times for water moving from the surface to the mine interior must be of the order of weeks or months. Knowledge of travel times may be useful for linking the chemistries of waters flowing into the tunnel with those of isolated rain and surface runoff events.

5.3 Chemistry of Waters in the Apache Leap Tuff

Table 20 gives chemical analyses of water samples taken from the Apache Leap Tuff. Apache Leap waters tend to be of intermediate pH and dominant in calcium and bicarbonate. Four of five tunnel samples (all except T-6340, located directly below Queen Creek) are at or near equilibrium with calcite and amorphous silica, the predominant fracture filling minerals identified in the system, thus alkalinity and silica concentrations are relatively constant. T-6340 is undersaturated with respect to both minerals.

Table 20: Analyses of water samples taken from Magma "Never-Sweat" haulage tunnel (500-Level). All samples collected on 7/6/89.

Property/ Constituent	T-CB1	T-CB2	T-4	T-7920	T-6340
T (C)	25.1	25.1	21.0	21.9	20.5
pH	7.85	7.76	7.55	7.79	7.40
Alkalinity (mg/l HCO3)	138.5	136.1	132.7	137.4	98.3
Silica (mg/l SiO2)	62.4	62.2	65.0	60.0	46.8
SO4 (mg/l)	15.6	15.7	60.8	7.8	32.2
NO3 (mg/l)	3.9	4.2	27.6	3.6	3.9
Cl (mg/l)	6.0	6.3	17.0	5.3	4.5
F (mg/l)	0.26	0.26	0.25	0.31	0.24
Br (mg/l)	0.07	0.06	0.08	0.05	0.05
Na (mg/l)	22.5	22.8	30.1	29.1	18.4
K (mg/l)	0.89	0.90	1.15	0.64	0.78
Ca (mg/l)	28.0	27.5	46.6	20.5	26.3
Mg (mg/l)	5.2	5.0	8.3	4.0	4.6

Other chemical constituents vary considerably among samples taken from different sites. Variations may be the function of several factors. Those that most likely differentiate waters in the tuff are discussed below. Waters in the tuff have entered a fracture flow system with a unique chemistry. The chemistry of surface runoff varies according to factors such as chemistry of precipitation, volume and duration of runoff event, length of time between events, and extent of transpiration. Comparison of chemical analyses for Queen Creek samples taken at different times illustrates surface runoff variability (Table 21).

Table 21: Chemical analyses of waters in the Apache Leap region.

Property/ Constituent	East End Tunnel (1) 9-11-78	Queen Creek Surface (2) 4-69	8-62
pH	7.5	-	-
Alkalinity (mg/l HCO_3)	138	88	176
Silica (mg/l SiO_2)	62		
SO4 (mg/l)	11	76	7
NO3 (mg/l)	-	< 1	< 1
Cl (mg/l)	6.7	6	6
F (mg/l)	-	0.11	0.3
Na (mg/l)	-	7	17
Ca (mg/l)	28.8	32	36
Mg (mg/l)	5.1	13	8

NOTES:

(1) Data provided by Magma Copper Company, Superior, AZ
(2) Data provided by Arizona Water Company, Superior, AZ

Variable mass of mineral dissolution/alteration likely controls the concentrations of most chemical constituents. Water-rock contact time is an important factor here. Waters react with primary tuff minerals (plagioclase, quartz, biotite, potassium feldspar, cristobalite) whereby minerals are dissolved or altered, releasing constituents into the aqueous system.

Some waters may have attained chemical equilibrium with minerals in the system while others, certainly, are too new in the environment to have achieved the more stable chemistry. Those waters most distant from a water source or traveling more slowly are most likely in equilibrium with minerals in the flow system. A fourth contributing factor may be variability of flow system chemical environments. Tuff mineralogy may deviate locally as will secondary mineralization within fractures. Variability of carbon dioxide partial pressure may be significant as well.

Comparison of recent chemical analyses to one performed 11 years earlier suggests that the chemistry of waters at the eastern end of the tunnel has remained relatively constant over time. Analyses for samples T-CB1 and T-CB2 collected in July, 1989, are very similar to an analysis done by Magma Copper Company in 1978. Chemical processes in the aqueous system have progressed sufficiently to attenuate initial chemical variations of waters entering the system. The aqueous chemistry at this site may represent a chemical average, brought about by mixing of waters moving through different fracture systems or the chemistry may be a chemical equilibrium for that aqueous system.

5.4 Analysis of Sulfate Concentrations Near a Fracture

An understanding of the interaction between flow through fractures and that through an unsaturated matrix is far from complete. Certainly some interaction occurs in unsaturated fractured rock systems, but the extent and mechanisms involved are unclear. A tracer found in water flowing through a system could be a useful tool for understanding interaction processes. Such a tracer may have been a constituent of water flowing through rocks in the region of the Apache Leap Site.

Between the years 1924 and 1972 a copper smelter was operated in Superior, Arizona, 3.1 km from Apache Leap Site. Hundreds of tons of sulfur, as sulfur dioxide gas, were emitted daily from its stacks. It is a reasonable assumption that a portion of this sulfur was carried to the ground surface near Apache Leap Site by wet and dry fallout and incorporated into runoff during precipitation events. If indeed this was the case, waters moving through the Apache Leap Tuff contained elevated sulfate concentrations compared to post-1972 and pre-1924 levels. If precipitated along a flow path, this sulfate of unusually high concentration could serve as a tracer in fracture flow/matrix flow interaction studies.

The experiment described here is a preliminary examination of relative sulfate concentrations at variable distances from a fracture that is water bearing during times of runoff availability. As a survey, objectives are to gain a general understanding about trends and to obtain data useful in the design of future experiments.

A fracture suitable for study was chosen based upon accessibility and its relative capacity to hold and transmit water. The fracture selected is in the White Unit of the tuff, 400 m southeast Apache Leap Site, trending N-S and dipping about 80° west. Rock samples were taken at variable horizontal, near perpendicular distances from the fracture. By drilling 45 cm

into the rock face parallel to the fracture with a hand held power drill, each sample was taken as rock fragments of uniform distance from the fracture.

After drying and grinding samples to a uniform grain size, hot water soluble sulfate was removed from the rock by elution in a beaker of pure water placed on a heat source for one hour. Preliminary experiments indicate that solubility of sulfate minerals present in the tuff increases with temperature and that a one hour elution time is sufficient to maximize dissolution. The resultant solution was cooled, centrifuged, filtered, and analyzed for sulfate concentration by ion chromatography. Water soluble sulfate concentrations of each rock sample were calculated from the data.

Figure 12 graphically represents the results of this study. Soluble sulfate concentrations are lowest at the fracture and increase in both directions away from the fracture. The gradient to the west is smooth, about 0.30 $\mu g\ g^{-1}\ cm^{-1}$, and concentrations reach a maximum at 11 cm from the fracture, then decline at a more gentle rate. To the east the trend is of increasing concentrations but the gradient is less discernible because of fewer data points. It is important to note that all values are useful for comparison purposes only. Concentration values do not represent absolute concentrations of sulfate in any form, but are the concentrations of sulfate eluted from rock samples by a precise procedure repeated uniformly for each sample.

An important assumption inherent in any interpretation linking sulfate concentration trends to flow patterns is that sulfate minerals in the rock are uniformly soluble within the sampled volume such that experimental concentration gradients reflect actual concentration gradients and not solubility gradients. A second assumption is that soluble sulfate in the rock originated from precipitation of sulfate minerals out of meteoric water and not from alteration of sulfide minerals. Apache Leap Tuff contains no sulfide mineral as a major constituent, but the presence of unidentified trace sulfides is possible. The smooth nature of the experimental concentration gradient suggests, however, that this is not the case because interception of sparse sulfur bearing minerals would likely generate an erratic concentration pattern.

Logical additional research may investigate the repeatable nature of the observed soluble sulfate concentration distribution. Since only one fracture was studied, it is not known if the observed trend is representative of more than one fracture. Modification of sulfate extraction techniques such that the degree of sulfate removal may be determined and controlled could further contribute to research into this area.

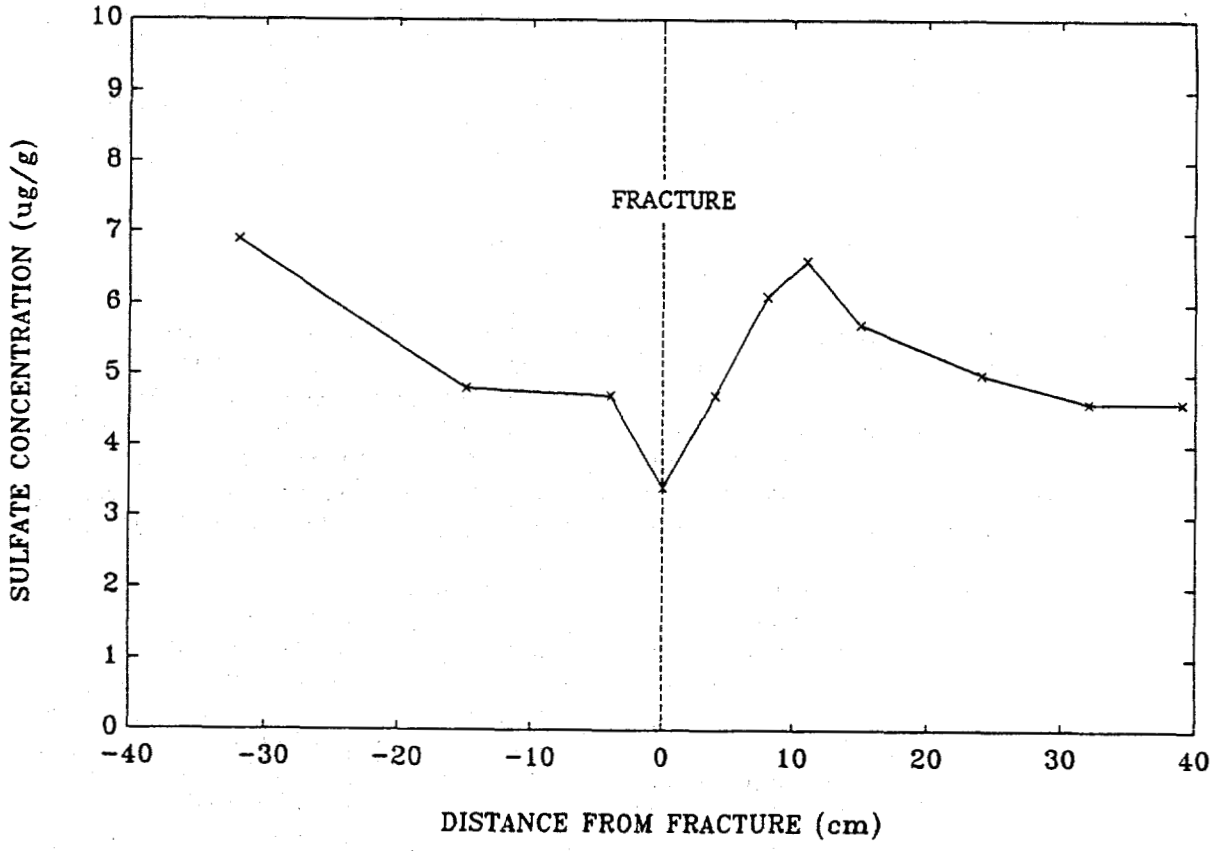

Figure 12: Hot water soluble sulfate concentrations in tuff samples taken at various distances from a fracture.

6. THERMOHYDROLOGIC EXPERIMENTS

To evaluate the relative importance of various impacts of heat generation within unsaturated fractured rock, as well as to provide preliminary data sets for evaluating the computer programs discussed above, a series of nonisothermal hydrologic laboratory and field experiments have been conducted. This section discusses two such experiments, a one-dimensional laboratory core heating experiment and a field heating experiment in fractured tuff.

6.1 Core Heater Experiment

Davies (1987) studied water movement within three unsaturated welded tuff cores in response to imposed thermal gradients of approximately 5 K cm^{-1}. These experiments consist of applying a thermal gradient along the long axis of unsaturated, unfractured tuff cores sealed and insulated from the environment with dimensions of approximately 10 cm in diameter and a length of approximately 30 cm (Figure 13). Real time monitoring of water flow as both liquid and vapor, as well as the solute and heat flow within the rock cores is made possible using gamma ray attenuation methods in conjunction with thermistors placed along the length of the cores. Bulk density and initial, transient and final water content distributions were determined each 1-cm along the cores using gamma attenuation methods. Temperatures within the cores were measured by thermocouples embedded 1.5 cm into the rock cores. Liquid return flow toward the heat source was demonstrated by the initial and final distributions of iodide (Figure 14). These experiments indicated that a countercurrent of water vapor driven away from a heat source and subsequent liquid return flow can be established when a thermal gradient is present within sealed porous rock cores.

6.2 Field Heater Experiment

A proposed field heater experiment has been evaluated to determine the effects of a thermal source on the movement of water as liquid and vapor. The thermal, hydraulic, and pneumatic properties of the rock matrix at the proposed heater experiment site have been determined from core samples collected at ALTS. The topography of the proposed heater site is presented as Figure 15. The spatial distribution and orientation of fractures at the proposed location have also been mapped (Figure 16).

A surface survey of the electrical resistivity properties of the proposed heater site is in progress. The water content of the volcanic tuff is the primary conductor of electrical current so that when the flow path is interrupted by one or more drained fractures the bulk or apparent resistivity increases. Five resistivity profiles, 60 to 80 m long, have been completed, providing spatial coverage of the knoll (Figure 16). Data are collected at electrode spacings of one and two meters, with the wider array penetrating to greater depths (Figure 17).

Preliminary results indicate that bulk resistivity increases with topographic elevation and with fracture density and magnitude (e.g., with the regional extent of the fracture trace). The location of fractures using

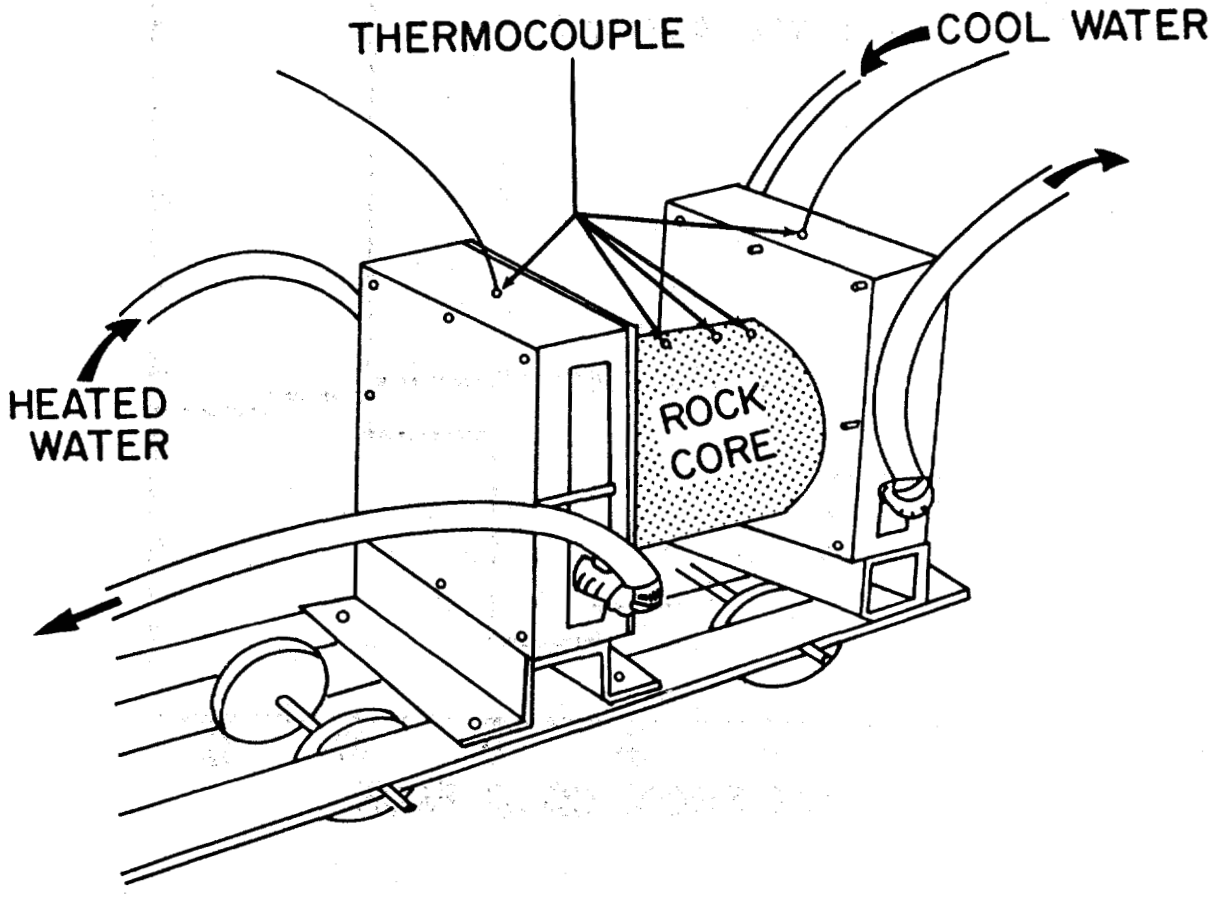

Figure 13: Diagram of apparatus used to conduct core heating experiments in unsaturated Apache Leap tuff.

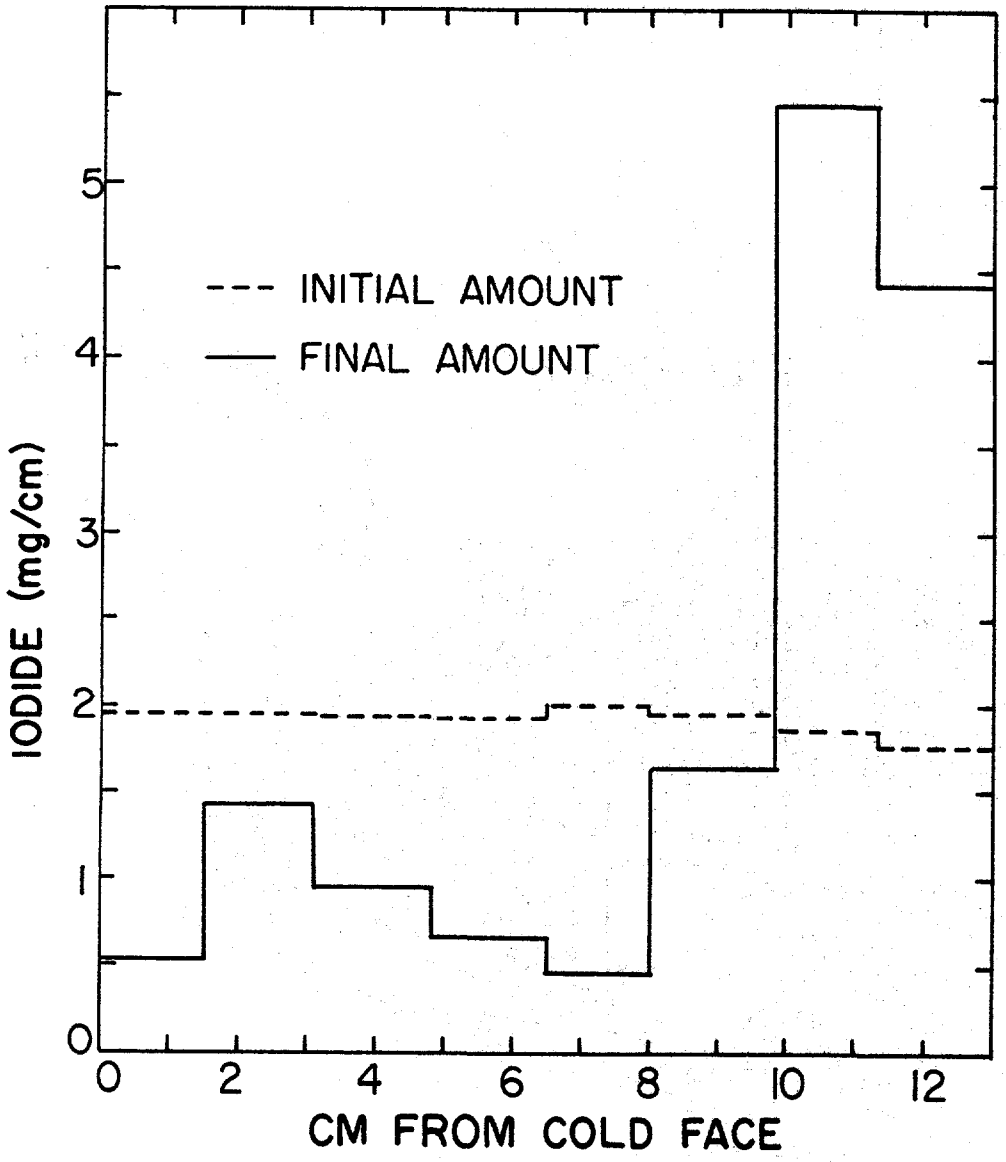

Figure 14: Initial and final solute concentration in unsaturated Apache Leap tuff core resulting from heating experiment.

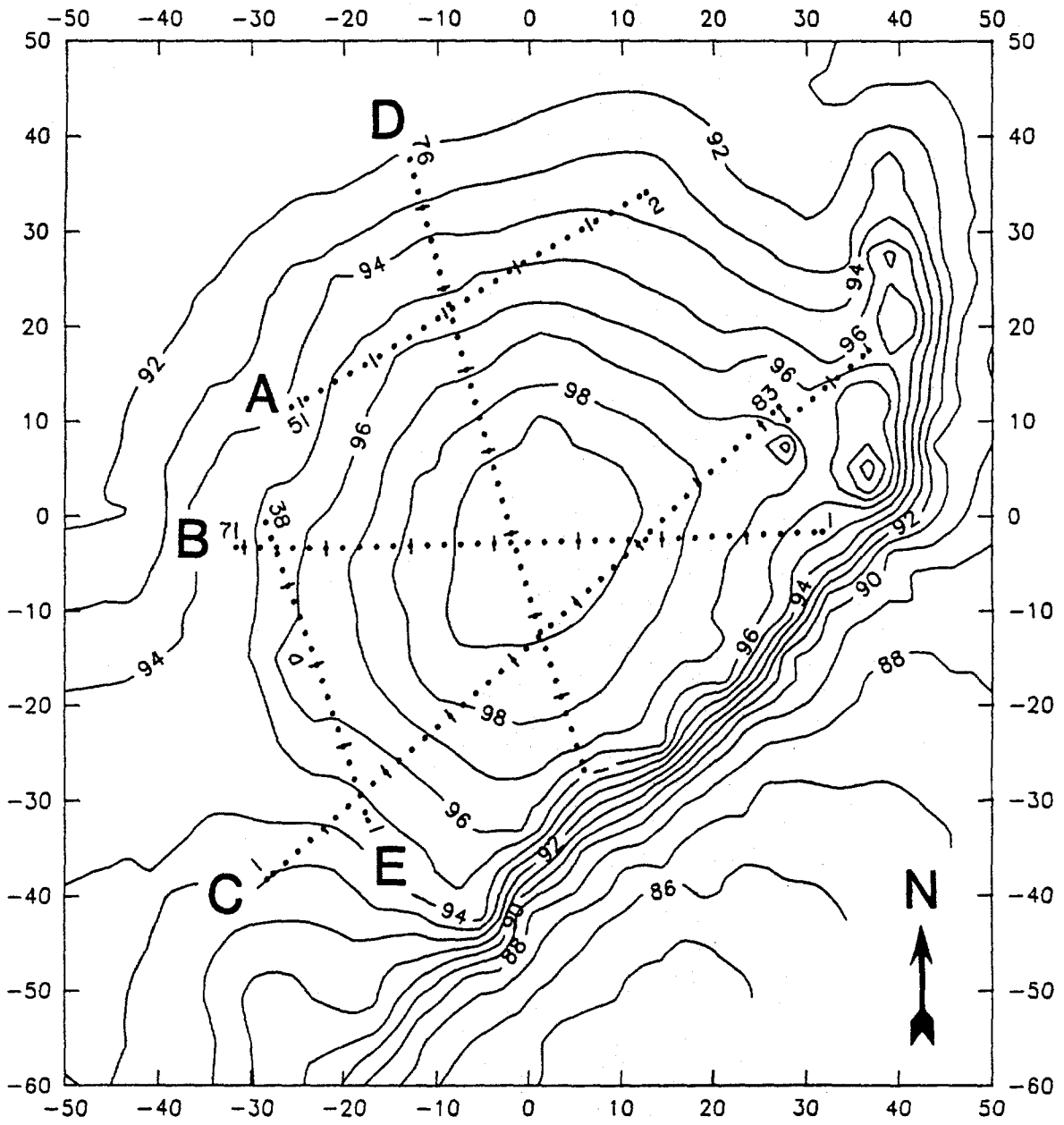

Figure 15: Topography of heater site showing locations of electrical resistivity profiles. Contour interval is one meter. Horizontal scale is in meters.

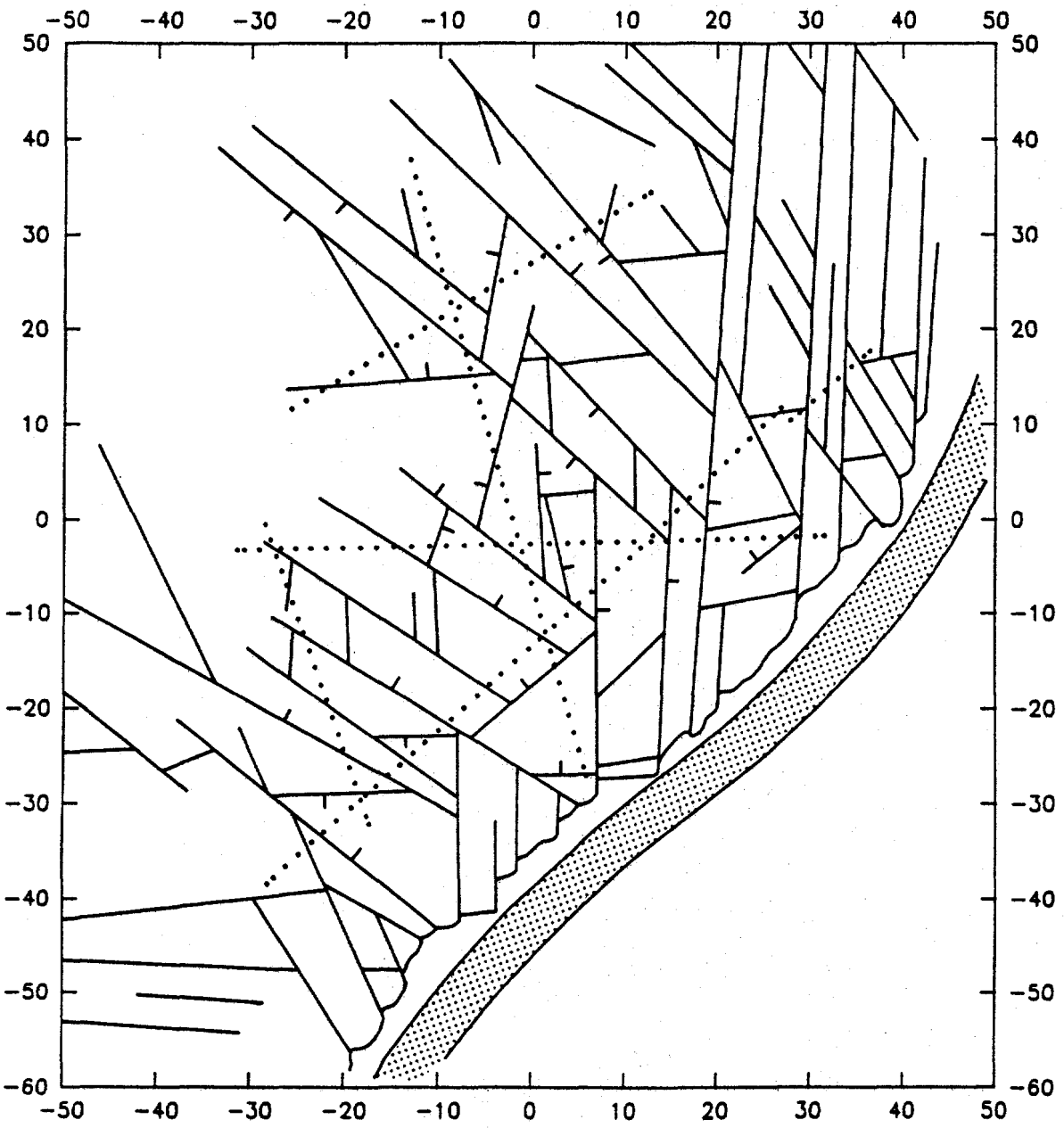

Figure 16: Structural lineaments interpreted from aerial photographs of fracture planes exposed in outcrop at heater site.

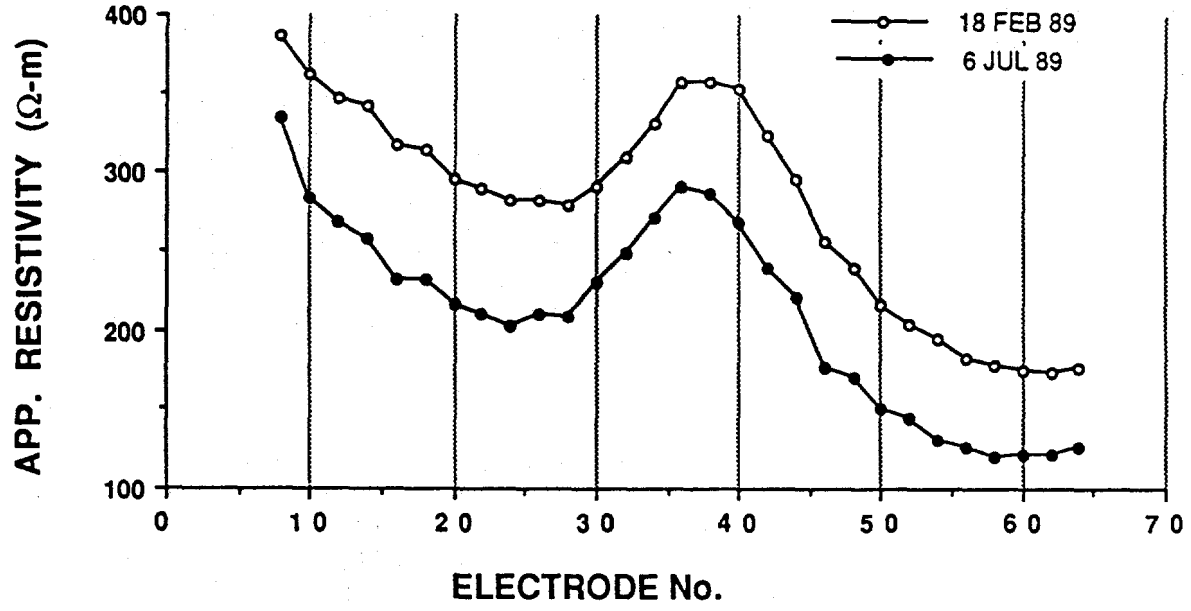

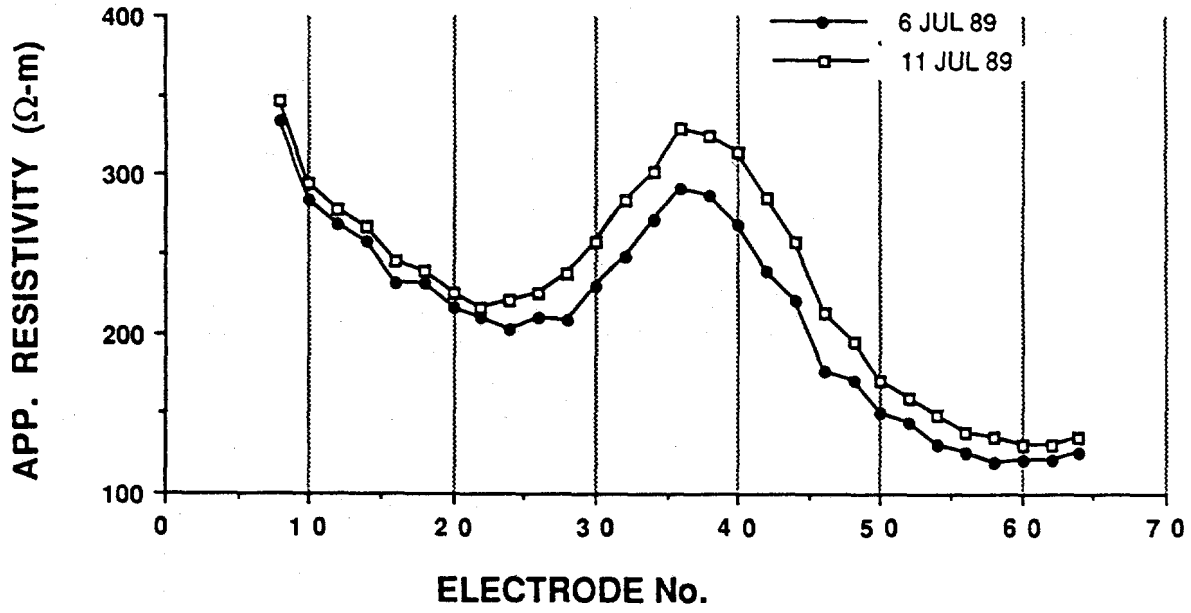

Figure 17: Electrical resistivity along B profile. Electrode spacing (horizontal axis) is one meter, and profiles depicted here were collected at two meter spacings, with an assumed penetration depth of approximately one meter. Profiles of upper diagram were surveyed under dry conditions, the difference between dates attributed to temperature effects on pore-fluid resistivity. Profiles of lower diagram were collected before and after a 12 mm rainfall event.

electrical methods correlates well with fracture trace images on areal photographs and field structural maps. Resistivity appears to decrease with depth as saturation increases. Laboratory measurements of electrical resistivity were conducted on cores of the volcanic tuff at different porosities and degrees of saturation. Such data quantify the relationship between resistivity and water content. Additional studies include monitoring the electrical response to an advancing wetting front during rainfall infiltration events, and the subsequent drainage of the fracture. Correlation of the electrical resistivity properties with cross-borehole ground-penetrating radio frequency surveys should also be used to complement surface surveys.

Using this information along with other estimated parameters, the TOUGH code is used to simulate water and vapor flows under various scenarios. The purpose of the simulations is to investigate the effects of the fracture distribution, thermohydrologic parameters, initial and boundary conditions, and strength and placement of the heater on liquid-vapor movement at the site. The simulations are necessary to guide the design of the future heater experiments. Preliminary simulations indicate that thermohydrologic conditions in the vicinity of the heater will depend strongly on relative permeability and suction characteristics of the fractures, which are poorly known at the present time. If liquid held on the rough walls of drained fractures is assumed to be mobile, strong heat pipe effects are predicted. If it is assumed that liquid cannot move along drained fractures, then the region surrounding the heater is predicted to dry out and formation temperature can rise significantly. Furthermore, simulations also show that vertical fractures can serve as conduits for vapor flow and can significantly affect the development of a heat pipe region near the heater.

Based on these results, we suggest that the future heater experiment should be conducted at locations where the fracture distribution is well-defined. Fractures connected to the heater location are the primary conduits for vapor flow; sensors for vapor should be placed along these fractures. Vertical fractures may affect lateral movements of vapor, liquid, and heat even if they do not intersect the heat source. Monitoring devices need to be installed close to the heater to determine whether the vertical fractures affect flows. Furthermore, an accurate estimate of initial moisture distribution at the vicinity of the heater location will be necessary.

REFERENCES

Bixler, N.E., 1985, "NORIA - A Finite Element Computer Program for Analyzing Water, Vapor, and Energy Transport in Porous Media", SAND84-2057, 115 pp.

Brown, S.R., 1986, "Unconfined Aquifer Recharge from Water Table Configuration Modeling", M.S. Thesis, University of Arizona.

Carslaw, H.S. and J.C. Jaeger, 1959, Conduction of Heat in Solids, Clarendon Press, 510 pp.

Chuang, Y., W.R. Haldeman, T.C. Rasmussen, and D.D. Evans, 1990, "Laboratory Analysis of Fluid Flow and Solute Transport Through a Variably Saturated Fracture Embedded in Porous Tuff", NUREG/CR-5482.

Davies, Bill, 1987, "Measurement of Thermal Conductivity and Diffusivity in an Unsaturated, Welded Tuff", M.S. Thesis, University of Arizona.

Elder, Alexander N., 1988, "Theoretical Calibration of Neutron Gauges", M.S. Thesis, University of Arizona.

Goering, Tim, 1988, "Use of Fluorescent Dyes as Tracers in Unsaturated, Fractured Rock", M.S. Thesis, University of Arizona.

Green, R.T. and D.D. Evans, 1987, "Radionuclide Transport as Vapor Through Unsaturated Fractured Rock", NUREG-CR-4654, 163 pp.

Hadley, G.R., 1985, "PETROS - A Program for Calculating Transport of Heat, Water, Vapor, and Air Through a Porous Material", SAND84-0878, 67 pp.

Haldeman, W.R., Y. Chuang, T.C. Rasmussen, and D.D. Evans, 1989, "Boundary Integral Method Applied to Steady Fluid Flow and Travel Times in Fractured Rock: 2. Coupled Fracture-Matrix Flow", Submitted to Water Resour. Res.

Myers, K.C., 1989, "Water Flow and Transport Through Unsaturated Discrete Fractures in Welded Tuff", M.S. Thesis, University of Arizona.

Oster, C.A., 1982, "Review of Ground-Water Flow and Transport Models in the Unsaturated Zone", NUREG/CR-2917, 160 pp.

Peterson, D.W., 1961, "Dacitic Ash-Flow Sheet Near Superior and Globe, Arizona", Ph.D. Dissertation, Stanford University, Palo Alto, CA.

Pruess, K., 1987, "TOUGH User's Guide", NUREG/CR-4645, 78 pp.

Rasmussen, T.C., 1987, "Computer Simulation of Steady Fluid Flow and Solute Transport Through Three-Dimensional Networks of Variably Saturated, Discrete Fractures", in Flow and Transport Through Unsaturated Fractured Rock, AGU Geophys. Monograph 42, p. 107-114.

Rasmussen, T.C. and D.D. Evans, 1987, "Unsaturated Flow and Transport Through Fractured Rock - Related to High-Level Waste Repositories", NUREG/CR-4655, 474 pp.

Rasmussen, T.C, T.-C.J. Yeh, and D.D. Evans, 1988, "Effect of Variable Fracture Permeability/Matrix Permeability Ratios on Three-Dimensional Fractured Rock Hydraulic Conductivity", in Geostatistical, Sensitivity, and Uncertainty Methods for Ground-Water Flow and Radionuclide Transport Modeling, by B.E. Buxton (ed.), Battelle Press, p. 337-358.

Rasmussen, T.C., 1989, "Boundary Integral Method Applied to Steady Fluid Flow and Travel Times in Fractured Rock: 1. Partially Saturated Fractures", Submitted to Water Resour. Res.

Rasmussen, T.C. and D.D. Evans, 1989, "Fluid Flow and Solute Transport Modeling Through Three-Dimensional Networks of Variably Saturated Discrete Fractures", NUREG/CR-5239.

Rasmussen, T.C., D.D. Evans, P.J. Sheets, and J.H. Blanford, 1990, "Unfractured Fractured Rock Characterization Methods and Data Sets at the Apache Leap Tuff Site", NUREG/CR-5596.

Rasmussen, T.C., J.H. Blanford, and P.J. Sheets, 1990, "Characterization of Unsaturated Fractured Tuff at the Apache Leap Site: Comparison of Laboratory/Field, Matrix/Fracture, and Water/Air Flow Data", in FOCUS '89: Proceedings of Nuclear Waste Isolation in the Unsaturated Zone, Amer. Nucl. Soc., p. 365-372.

Rogoff, E.B., 1988, "Characterization of Water Interaction with the Apache Leap Tuff, Superior, Arizona, Using Stable Isotopes of Oxygen and Hydrogen", M.S. Thesis, University of Arizona, Department of Hydrology and Water Resources.

Smith, S.J., 1989, "Natural Airflow Through the Apache Leap Tuff near Superior, Arizona", M.S. Thesis, University of Arizona.

Tidwell, V.C., 1988, "Determination of the Equivalent Saturated Hydraulic Conductivity of Fractured Rock Located in the Vadose Zone", M.S. Thesis, University of Arizona.

Tidwell, V.C., T.C. Rasmussen, and D.D. Evans, 1988, "Saturated Hydraulic Conductivity Estimates for Fractured Rock in the Unsaturated Zone", Validation of Flow and Transport Models for the Unsaturated Zone, Ruidoso, N.M., NMSU, p. 414-421.

Tien, P.-L., M.D. Siegel, C.D. Updegraff, K.K. Wahi, and R.V. Guzowski, 1985, "Repository Site Data Report for Unsaturated Tuff, Yucca Mountain, Arizona", NUREG/CR-4110.

Vogt, Gerald T., 1988, "Porosity, Pore-Size Distribution and Pore Surface Area of the Apache Leap Tuff near Superior, Arizona Using Mercury Porosimetry", M.S. Thesis, University of Arizona.

Weber, D.S. and D.D. Evans, 1988, "Stable Isotopes of Authigenic Minerals in Variably-Saturated Fractured Tuff", NUREG/CR-5255.

Yeh, T.C.J., T.C. Rasmussen and D.D. Evans, 1988, "Simulation of Liquid and Vapor Movement in Unsaturated Fractured Rock at the Apache Leap Tuff Site: Models and Strategies", NUREG/CR-5097, 73 pp.

NRC FORM 335 (2-89) NRCM 1102, 3201, 3202

U.S. NUCLEAR REGULATORY COMMISSION

BIBLIOGRAPHIC DATA SHEET

(See instructions on the reverse)

1. REPORT NUMBER (Assigned by NRC. Add Vol., Supp., Rev., and Addendum Numbers, if any.)

NUREG/CR-5581

2. TITLE AND SUBTITLE

Unsaturated Flow and Transport Through Fractured Rock Related to High-Level Waste Repositories

Final Report -- Phase III

3. DATE REPORT PUBLISHED

MONTH: January YEAR: 1991

4. FIN OR GRANT NUMBER

FIN D1662

5. AUTHOR(S)

Daniel D. Evans and Todd C. Rasmussen

6. TYPE OF REPORT

Final Technical

7. PERIOD COVERED *(Inclusive Dates)*

Aug 1986 - Dec 1989

8. PERFORMING ORGANIZATION – NAME AND ADDRESS *(If NRC, provide Division, Office or Region, U.S. Nuclear Regulatory Commission, and mailing address; if contractor, provide name and mailing address.)*

Department of Hydrology and Water Resources
University of Arizona
Tucson, AZ 85721

9. SPONSORING ORGANIZATION – NAME AND ADDRESS *(If NRC, type "Same as above"; if contractor, provide NRC Division, Office or Region, U.S. Nuclear Regulatory Commission, and mailing address.)*

Division of Engineering
Office of Nuclear Regulatory Research
U.S. Nuclear Regulatory Commission
Washington, DC 20555

10. SUPPLEMENTARY NOTES

11. ABSTRACT *(200 words or less)*

Research results are summarized for a U.S. Nuclear Regulatory Commission contract with the University of Arizona focusing on field and laboratory methods for characterizing unsaturated fluid flow and solute transport related to high-level radioactive waste repositories. Characterization activities are presented for the Apache Leap Tuff field site. The field site is located in unsaturated, fractured tuff in central Arizona. Hydraulic, pneumatic, and thermal characteristics of the tuff are summarized, along with methodologies employed to monitor and sample hydrologic and geochemical processes at the field site. Thermohydrologic experiments are reported which provide laboratory and field data related to the effects of non-isothermal conditions and flow and transport in unsaturated, fractured rock.

12. KEY WORDS/DESCRIPTORS *(List words or phrases that will assist researchers in locating the report.)*

Fractured Rock, Vadose Zone, Unsaturated Zone, Solute Transport

Contaminant Transport, High-Level Nuclear Waste

13. AVAILABILITY STATEMENT

Unlimited

14. SECURITY CLASSIFICATION

(This Page) Unclassified

(This Report) Unclassified

15. NUMBER OF PAGES

16. PRICE